Available online www.ejaet.com

European Journal of Advances in Engineering and Technology, 2025, 12(4):28-56

Research Article ISSN: 2394 - 658X

Numerical Modelling of Two-dimensional Wind and Pressure Fields for Hurricane Mitch (1998) in the Caribbean Sea – The Second Deadliest Tropical Hurricane in the Atlantic Basin

Md Akhtaruzzaman Sarker (PhD)

Technical Director, Royal HaskoningDHV, Westpoint, Peterborough Business Park, Lynch Wood, Peterborough PE2 6FZ, United Kingdom.
E-mail: zaman.sarker@rhdhv.com

ABSTRACT

Tropical hurricanes (also known as cyclones or typhoons) cause significant loss of life and damage to properties, marine facilities and ecosystems. Climate change is likely to worsen the problem. Hurricane modelling results are used for deriving robust design conditions for coastal and marine structures and facilities. These are also used for emergency planning and decision-making to estimate potential loss of life, damage to properties and marine facilities and to develop rescue and mitigation measures and plan for clean-up operations. Sufficient information on the deadliest hurricane in the Atlantic Basin (Great Hurricane, 1780) is not available to carry out numerical modelling studies whereas some information on the second deadliest tropical hurricane (Hurricane Mitch, 1998) is available. Therefore, Hurricane Mitch was selected for further studies in this paper to provide additional information. Raw data (such as track, wind speed and central pressure) were obtained from IBTrACS. Radius of maximum wind speed was not available from IBTrACS and was, therefore, calculated following Quiring et al. (2011). Two-dimensional wind and pressure fields along the entire track of the hurricane were then generated using the Cyclone Wind Generation Tool of DHI. Two-dimensional wind and pressure fields at selected locations along the track of the hurricane are presented in this paper. Time-series wind speed and pressure over the entire passage of the hurricane are also provided at these selected locations. These wind and pressure fields are useful for numerical modelling of waves and surge. Structural design considerations and hurricane risk reduction measures are also provided in this paper. The methodology described in this paper for generating wind and pressure fields from Hurricane Mitch could also be applied for other hurricanes around the world.

Keywords: Natural Hazards, Cyclones, Hurricanes, Typhoons, Hurricane Mitch, Port Development, Royal HaskoningDHV.

INTRODUCTION

Formation of Hurricanes

Tropical hurricanes (also known as typhoons or cyclones) are associated with warm and moist air and hence they form only over warm ocean waters near the equator (within latitude 30° north and south). They need some favourable conditions to form such as:

a) Warm sea surface temperature;
b) Large convective instability;
c) Low level positive vorticity;
d) Weak vertical wind shear of horizontal wind; and
e) Coriolis force.

Warm ocean waters of at least 26.5°C throughout a depth of about 50m from sea surface is required for hurricane formation. The warm and moist air rises causing an area of lower pressure beneath. Cooler air moves into the lower pressure area and becomes warm and moist and rises too. When the warm and moist air rises, it cools down and forms clouds. The entire system of clouds and winds spins and grows and is fed by ocean's heat and evaporated water continuously. Hurricanes that form north of the equator spin counterclockwise whereas hurricanes south of the equator spin clockwise due to the difference in Earth's rotation on its axis.

Storm surges from hurricanes are generated due to an interaction between air and water. The atmosphere forces the water body and consequently oscillations are generated in the water body with periods ranging from a few minutes to a few days. A hurricane becomes deadly by causing inundation along the coastline if the maximum surge coincides with a high astronomical tide.

There are essentially two major forcing factors when a weather system moves over a water body:

a) Atmospheric pressure gradient normal to the sea surface. This is known as “inverse barometer effect” or “static amplification” or “static part of the storm surge”. A decrease of one hectopascal (hPa) in the atmospheric pressure raises the sea level by one centimeter (cm). This static part has only about 5-15% contribution in the magnitude of a surge.

b) The dominant factor, known as “dynamic amplification”, is caused by the tangential wind stress (associated with the wind field of the weather system) acting over the sea surface which pushes the water towards the coast resulting to a pile-up of water at the coast.

The Saffir-Simpson Hurricane Wind Scale

The well-known Saffir-Simpson Hurricane Wind Scale [1] is designed to help determine wind hazards of an approaching hurricane easier for emergency officials. The scale is assigned five categories with Category 1 assigned to a minimal hurricane and Category 5 to a worst-case scenario. The Saffir-Simpson Scale classifying hurricane Category 1 to 5 is given in Table 1 [1]. Conditions for tropical depression and tropical storm are also provided in the table.

Table 1: Saffir-Simpson Hurricane Classification [1]

Storm type	Category	Minimum pressure (hPa, mb)	1-minute maximum sustained wind speed				Surge (m)	Damage
			knots	mph	km/h	m/s		
Tropical Depression	TD	-	< 34	<39	< 63	0-17	0	-
Tropical Storm	TS	-	34 – 63	39 – 73	63 – 118	18-32	0-0.9	-
Hurricane	1	> 980	64 – 82	74 – 95	119 – 153	33-42	1.0-1.7	Minimal
Hurricane	2	965 – 980	83 – 95	96 – 110	154 – 177	43-49	1.8-2.6	Moderate
Hurricane	3	945 – 965	96 – 113	111 – 130	178 – 210	50-58	2.7-3.8	Extensive
Hurricane	4	920 – 945	114 – 135	131 - 155	211 - 250	59-69	3.9-5.6	Extreme
Hurricane	5	< 920	> 135	> 155	> 250	>70	>5.7	Catastrophic

Damages from Hurricanes

Hurricanes are associated with high-pressure gradients and consequently generate strong winds, torrential rain and storm surges at landfall making these one of Earth’s most destructive natural phenomena. The destruction from a tropical hurricane depends on its intensity, size and location. Very strong winds may damage installations, dwellings, transportation and communication systems, trees etc. and cause fires resulting in considerable loss of life and damage to property and ecosystems. Hurricanes also impose significant risks during construction and operation of seaports and other marine structures and facilities.

Hurricanes have been responsible for the deaths of about 1.9 million people worldwide during the last two centuries. It is estimated that 10,000 people per year perish due to tropical cyclones [2]. Bangladesh is especially vulnerable to tropical cyclones with around 718,000 deaths from them in the past 50 years [3]. The deadliest tropical cyclone in Bangladesh was Cyclone Bhola (1970), which had a death toll of at least 300,000 [4] possibly as many as 500,000 [5, 6]. An estimated over 138,000 people were killed [7] with an equal number of injured [8] and about 13.4 million people were affected [8] by the 1991 Cyclone in Bangladesh.

During the 50 years since Cyclone Bhola, 1942 disasters were attributed to tropical cyclones worldwide which killed 779,324 people and caused US$ 1,407.6 billion in economic losses with an average of 43 deaths and US$ 78 million in damages every day [9].

Maximum damages from a cyclone occur if landfall takes place at high tide. There was a severe cyclone in the Bay of Bengal in October 1960 which claimed only over 5,000 lives [10] although the strength of this cyclone was like that of Cyclone Bhola (November 1970). The significant difference in fatalities is because the November 1970 cyclone crossed the coast at high tide while the October 1960 storm moved onshore at low tide [11].

A list of deadliest Pacific typhoons is provided in Table 2 [12]. The August 1931 China typhoon killed 300,000 [13] as reported in [12]. Typhoon Nina in 1975 killed 229,000 [14] as reported in [12]. The costliest known Pacific typhoons (adjusted for inflation) are shown in Table 3 [15] as reported in [16]. Tables 4 and 5 show the deadliest [17] and the costliest [18] hurricanes in the Atlantic Ocean. A list of the deadliest cyclones in the Northern Indian Ocean is provided in Table 6 [17].

Table 2: Deadliest Pacific typhoons [12]

Rank	Typhoon	Season	Fatalities
1	August 1931 China typhoon	1931	300,000
2	Nina	1975	229,000
3	July 1780 Typhoon	1780	100,000
4	July 1862 Typhoon	1862	80,000
5	Shantou	1922	60,000
6	China	1912	50,000
7	Hong Kong	1937	10,000
8	Joan	1964	7,000
9	Haiyan	2013	6,352
10	Vera	1959	>5,000

Table 3: Costliest Pacific typhoons [15]

Rank	Typhoon	Season	Damage (2023 USD)
1	Doksuri	2023	$28.4 billion
2	Mireille	1991	$22.4 billion
3	Hagibis	2019	$20.6 billion
4	Jebi	2018	$17.0 billion
5	Yagi	2024	$16.5 billion
6	Songda	2004	$15.0 billion
7	Fitow	2013	$13.6 billion
8	Faxai	2019	$11.9 billion
9	Saomai	2000	$11.1 billion
10	Lekima	2019	$11.1 billion

Table 4: Deadliest Atlantic hurricanes [17]

Rank	Hurricane	Category	Season	Fatalities
1	Great Hurricane	?	1780	22,000–27,501
2	Mitch	5	1998	11,374+
3	Fifi	2	1974	8,210–10,000
4	Galveston	4	1900	8,000–12,000
5	Flora	4	1963	7,193
6	Pointe-à-Pitre	?	1776	6,000+
7	Okeechobee	5	1928	4,112+
8	Newfoundland	?	1775	4,000–4,163
9	Monterrey	3	1909	4,000
10	San Ciriaco	4	1899	3,855

Table 5: Costliest Atlantic hurricanes [18]

Rank	Hurricane	Category	Season	Damage
1	Katrina	5	2005	$125 billion
2	Harvey	4	2017	$125 billion
3	Ian	5	2022	$113 billion
4	Maria	5	2017	$91.6 billion
5	Irma	5	2017	$77.2 billion
6	Ida	4	2021	$75.3 billion
7	Sandy	3	2012	$68.7 billion
8	Ike	4	2008	$38 billion
9	Andrew	5	1992	$27.3 billion
10	Ivan	5	2004	$26.1 billion

Table 6: Deadliest cyclones in the Northern Indian Ocean [17]

Rank	Name/Year	Region	Fatalities
1	Bhola 1970	Bangladesh	>300,000
2	Unnamed 1582	Bangladesh	200,000
3	Unnamed 1876	Bangladesh	200,000
4	Unnamed 1897	Bangladesh	175,000

5	Bangladesh 1991	Bangladesh	138,866
6	Nargis 2008	Myanmar	138,373
7	Unnamed 1911	Bangladesh	120,000
8	Unnamed 1847	Bangladesh	75,000
9	Unnamed 1917	Bangladesh	70,000
10	Unnamed 1699	Bangladesh	50,000
11	Unnamed 1767	Bangladesh	50,000
12	Unnamed 1822	Bangladesh	50,000
13	Unnamed 1919	Bangladesh	40,000
14	Unnamed 1831	Bangladesh	22,000
15	Unnamed 1965	Bangladesh	19,270
16	Unnamed 1965	Bangladesh	12,000
17	Unnamed 1958	Bangladesh	12,000
18	Unnamed 1963	Bangladesh	11,520
19	Unnamed 1961	Bangladesh	11,468
20	Unnamed 1985	Bangladesh	11,069
21	Unnamed 1971	Bangladesh, India	11,000
22	Unnamed 1961	Bangladesh	10,466
23	Unnamed 1965	Pakistan	10,000
24	Unnamed 1977	India	10,000
25	Unnamed 1999	Bangladesh, India, Myanmar	9,899
26	Unnamed 1960	Bangladesh	8,149
27	Unnamed 1941	Bangladesh	7,000
28	Unnamed 1988	Bangladesh, India	6,240
29	Unnamed 1999	Pakistan	6,200
30	Unnamed 1960	Bangladesh	6,000

Benefits from Hurricanes

Despite their devastating effects, tropical hurricanes are essential features of the Earth's atmosphere as they bring rain to dry areas and transfer heat and energy from the equator to the cooler regions nearer the poles.

Impact of Climate Change on Hurricanes

The observed and the projected impacts of climate change on tropical cyclones presented in this section were obtained from the Intergovernmental Panel on Climate Change (IPCC) [19].

Past Observations [19]

Globally the frequency of tropical cyclones has not increased and in fact the number may have fallen. However, it is likely that a higher proportion of tropical cyclones across the globe are reaching category three or above meaning these reach the highest wind speeds. The frequency and magnitude of rapid intensification has likely increased. This is where maximum wind speeds increase very quickly which can be especially dangerous. In some places, the average location where tropical cyclones reach their peak intensity has shifted poleward exposing new communities to these hazards. There also seems to have been a slowdown in the speed at which tropical cyclones move across the Earth's surface. This typically brings more rainfall for a given location. There has been an increase in the average and peak rainfall rates associated with tropical cyclones. There is high confidence that humans have contributed to increases in precipitation associated with tropical cyclones and medium confidence that humans have contributed to the higher probability of a tropical cyclone being more intense.

Future Projections [19]

Rising temperatures affect tropical cyclones in several ways such as a) warmer ocean waters mean cyclones can pick up more energy leading to higher wind speeds b) a warmer atmosphere can hold more moisture leading to more intense rainfall and c) sea-levels are rising due to melting glaciers and ice sheets; storm surges from tropical cyclones on the top of already elevated sea levels worsen coastal flooding. The number of tropical cyclones globally is unlikely to increase. However, as the Earth warms, it is very likely that these will have higher rates of rainfall and reach higher top wind speeds. This means a higher proportion would reach the most intense categories four and five. The more global temperatures rise, the more extreme these changes will be. The proportion of tropical cyclones reaching categories four and five may increase by around 10% if global temperature rises are limited to 1.5°C, increasing to 13% at 2°C and 20% at 4°C.

Major Hurricanes in the Caribbean Sea

Hurricanes are one of the most frequent natural disasters that impact the Caribbean due to the high amounts of humidity and warm air produce near perfect conditions to form these hurricanes. Because of these favourable conditions, there have been many hurricanes that have passed through and affected the Caribbean waters. Figure 1 shows the tracks of tropical cyclones worldwide (1945–2006) [20]. The figure suggests that the Caribbean Sea is subjected to significant number of powerful hurricanes. Most notably hurricanes in the Caribbean Sea are provided in Table 7.

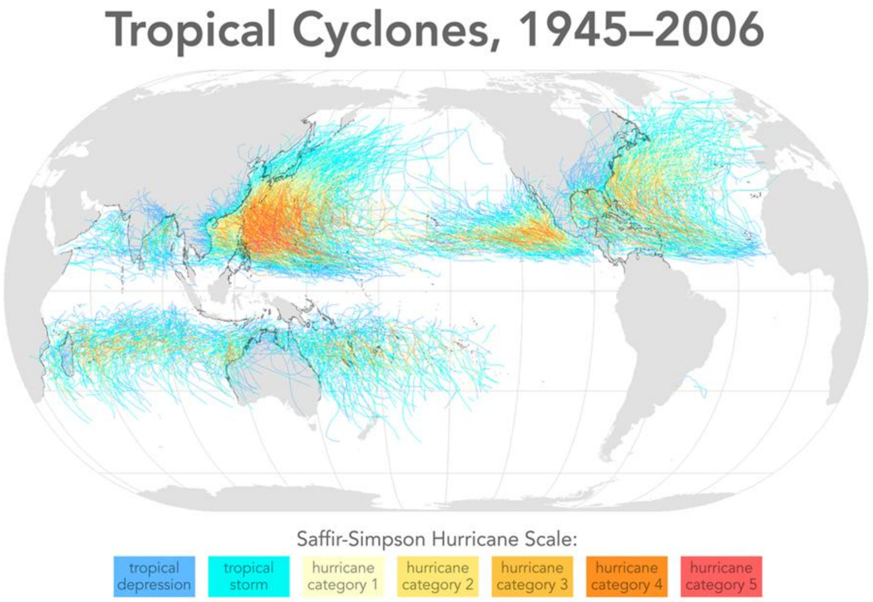

Figure 1: Tracks of tropical cyclones worldwide (1945–2006) [20]

Table 7: Most notable hurricanes in the Caribbean Sea [21]

Hurricanes	**Year**
The Great Hurricane	1780
San Ciriaco	1899
Hurricane Gilbert	1988
Hurricane Mitch	1998
Hurricane season	2008
Hurricane Sandy	2012
Hurricane Joaquin	2015
Hurricane Irma	2017

The Atlantic Hurricane Season runs from June to November and peaks from August to October [22]. The people of the Caribbean view hurricanes as a natural part of life. When a hurricane touches down on a Caribbean island the damage is substantial; the ecology is thrown out of its normal cycle, topography shifts, agriculture is set back, the economy and industry take a blow, society either unites or falls apart, infrastructure is ruined, and preventative measures must be implemented. There is no part of Caribbean life or its history that is untouched by natural disasters. As far back as Columbus, hurricane activity was recorded as he sailed across the Atlantic [23]. This extensive record of impacts influences Caribbean life and the people living in the Caribbean nations.

The Present Study

Hurricanes are one of the most frequent natural disasters that impact the Caribbean. Sufficient information on the deadliest hurricane in the Atlantic Basin (Great Hurricane, 1780) is not available to carry out numerical modelling studies whereas some information on the second deadliest tropical hurricane (Hurricane Mitch, 1998) is available. Therefore, Hurricane Mitch was selected for further studies in this paper to provide additional information.

Raw data (such as track, wind speed and central pressure) were obtained from IBTrACS [24]. Radius of maximum wind speed was not available from IBTrACS and was, therefore, calculated following Quiring et al. [25]. Two-dimensional wind and pressure fields along the entire track of the hurricane were then generated using the Cyclone Wind Generation Tool of DHI [26]. Two-dimensional wind and pressure fields at selected locations along the track of the hurricane are presented in this paper. Time-series wind speed and pressure over the entire passage of the hurricane are also provided at these selected locations.

The wind and pressure fields are useful for numerical modelling of waves and surge. Structural design considerations and hurricane risk reduction measures are also provided in this paper. The methodology described in this paper for generating wind and pressure fields from Hurricane Mitch could also be applied for other hurricanes around the world.

HURRICANE MITCH (1998)

Formation of Hurricane Mitch

Hurricane Mitch began as a tropical storm over the south-western Caribbean Sea on 22 October 1998 and strengthened to a hurricane by 24 October. Mitch then rapidly strengthened, becoming a monster Category 5 hurricane with a central pressure of 905 mb and maximum sustained winds of 180 mph (290 km/h) on 26 October. Mitch made landfall in Honduras as a much weaker Category 1 hurricane. After making landfall, Mitch eventually moved back into the Gulf of Mexico and headed toward Florida, making another landfall as a tropical storm. The above information was obtained from Wikipedia [27].

Damages from Hurricane Mitch

Hurricane Mitch was the second-deadliest tropical cyclone in the Atlantic basin on record. Mitch caused 11,374 fatalities in Central America, including approximately 7,000 in Honduras and 3,800 in Nicaragua due to cataclysmic flooding from the slow motion of the storm. It was the deadliest hurricane in Central American history. Mitch was the deadliest Atlantic hurricane in the satellite era, and the second-deadliest on record in the Atlantic, only behind the Great Hurricane of 1780 which killed at least 22,000 people. Deaths and damages from Hurricane Mitch by region are provided in Table 8 [27]. The above information was obtained from Wikipedia [27].

Table 8: Impact of Hurricane Mitch by region [27]

Region	Deaths	Damages
United States	2	$40 million
Panama	3	$50,000
Offshore	31	-
Nicaragua	3,800	$1 billion
Mexico	9	$1 million
Jamaica	3	Unknown
Honduras	7,000	$3.8 billion
Guatemala	268	$748 million
El Salvador	240	$400 million
Costa Rica	7	$92 million
Belize	11	$50,000
Total	11,374	$6.08 billion

Track and Data of Hurricane Mitch

The track (route) of Hurricane Mitch was obtained from [24, 28] and is shown in Figure 2. The hurricane data was obtained from IBTrACS [24]. The IBTrACS archived cyclone data contains 3-hourly information including date and time, track (path) and the maximum sustained wind speeds (1-minute mean). Data on Hurricane Mitch is provided in Table 9 [24]. Figure 3 shows the wind and central pressure intensity for Hurricane Mitch obtained from IBTrACS [24].

Figure 2a: Track of Hurricane Mitch (1998) [28]

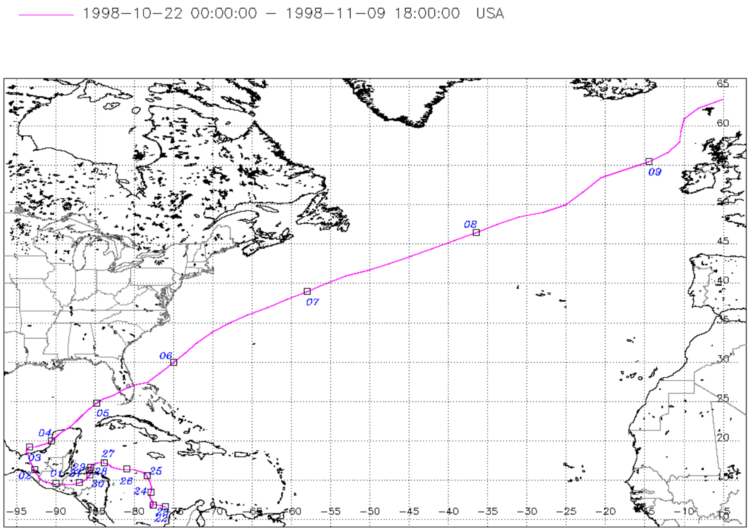

Figure 2b: Track of Hurricane Mitch (1998) [24]

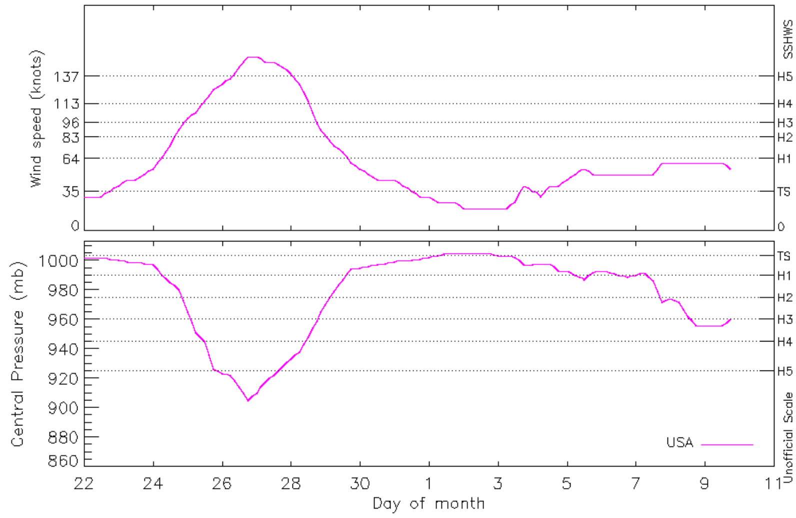

Figure 3: Wind and central pressure intensity plot of Hurricane Mitch (1998) [24]

Table 9: Track and data of Hurricane Mitch (1998) [24]

Date and Time [UTC]	Latitude [°N]	Longitude [°W]	Maximum 1-minute wind speeds [knots]	Central pressure [hPa]	Radius of maximum winds (estimated) [nm]
22/10/1998 00:00	11.6	-76.1	30	1002	42.5
22/10/1998 03:00	11.8	-76.6	30	1002	42.5
22/10/1998 06:00	11.9	-77.1	30	1002	42.5
22/10/1998 09:00	12.0	-77.6	30	1002	42.5
22/10/1998 12:00	12.0	-77.9	30	1002	42.5
22/10/1998 15:00	11.8	-78.0	33	1002	41.8
22/10/1998 18:00	11.6	-77.9	35	1001	41.3
22/10/1998 21:00	11.6	-77.8	38	1001	40.6
23/10/1998 00:00	11.8	-77.6	40	1000	40.1
23/10/1998 03:00	12.0	-77.6	43	1000	39.4
23/10/1998 06:00	12.2	-77.6	45	999	38.9
23/10/1998 09:00	12.4	-77.7	45	999	38.9
23/10/1998 12:00	12.5	-77.8	45	999	38.9
23/10/1998 15:00	12.7	-77.9	48	999	38.2
23/10/1998 18:00	12.9	-78.0	50	998	37.7
23/10/1998 21:00	13.1	-78.0	53	998	37.0
24/10/1998 00:00	13.4	-77.9	55	997	36.5

24/10/1998 03:00	13.6	-77.8	60	994	35.3
24/10/1998 06:00	13.9	-77.8	65	990	34.1
24/10/1998 09:00	14.2	-77.8	70	988	32.9
24/10/1998 12:00	14.5	-77.9	75	985	31.7
24/10/1998 15:00	14.8	-78.0	83	983	29.8
24/10/1998 18:00	15.0	-78.1	90	980	28.1
24/10/1998 21:00	15.2	-78.2	95	973	26.9
25/10/1998 00:00	15.5	-78.4	100	965	25.7
25/10/1998 03:00	15.8	-78.6	103	958	25.0
25/10/1998 06:00	16.0	-78.9	105	951	24.5
25/10/1998 09:00	16.1	-79.2	110	948	23.3
25/10/1998 12:00	16.2	-79.6	115	945	22.1
25/10/1998 15:00	16.3	-79.9	120	936	20.9
25/10/1998 18:00	16.4	-80.3	125	926	19.7
25/10/1998 21:00	16.4	-80.6	128	925	19.0
26/10/1998 00:00	16.4	-81.0	130	923	18.5
26/10/1998 03:00	16.4	-81.4	133	923	17.8
26/10/1998 06:00	16.4	-81.8	135	922	17.3
26/10/1998 09:00	16.5	-82.2	140	918	16.1
26/10/1998 12:00	16.6	-82.6	145	914	14.9
26/10/1998 15:00	16.7	-82.9	150	910	13.7
26/10/1998 18:00	16.9	-83.1	155	905	12.5
26/10/1998 21:00	17.1	-83.4	155	908	12.5
27/10/1998 00:00	17.2	-83.8	155	910	12.5
27/10/1998 03:00	17.3	-84.1	153	914	13.0
27/10/1998 06:00	17.3	-84.4	150	917	13.7
27/10/1998 09:00	17.2	-84.7	150	920	13.7
27/10/1998 12:00	17.1	-85.0	150	922	13.7
27/10/1998 15:00	17.0	-85.2	148	925	14.2
27/10/1998 18:00	16.9	-85.4	145	928	14.9
27/10/1998 21:00	16.8	-85.5	143	931	15.4
28/10/1998 00:00	16.6	-85.6	140	933	16.1
28/10/1998 03:00	16.4	-85.6	135	936	17.3
28/10/1998 06:00	16.3	-85.6	130	938	18.5
28/10/1998 09:00	16.3	-85.6	123	943	20.2
28/10/1998 12:00	16.3	-85.6	115	948	22.1
28/10/1998 15:00	16.3	-85.6	105	954	24.5
28/10/1998 18:00	16.3	-85.7	95	959	26.9
28/10/1998 21:00	16.3	-85.8	90	965	28.1
29/10/1998 00:00	16.2	-85.8	85	970	29.3
29/10/1998 03:00	16.2	-85.8	80	975	30.5
29/10/1998 06:00	16.1	-85.8	75	979	31.7
29/10/1998 09:00	16.0	-85.8	73	983	32.2
29/10/1998 12:00	15.9	-85.7	70	987	32.9
29/10/1998 15:00	15.9	-85.6	65	991	34.1
29/10/1998 18:00	15.8	-85.6	60	994	35.3
29/10/1998 21:00	15.7	-85.6	58	995	35.8
30/10/1998 00:00	15.6	-85.7	55	995	36.5
30/10/1998 03:00	15.5	-85.8	53	996	37.0
30/10/1998 06:00	15.4	-85.9	50	996	37.7
30/10/1998 09:00	15.3	-86.0	48	997	38.2
30/10/1998 12:00	15.2	-86.1	45	997	38.9
30/10/1998 15:00	15.0	-86.3	45	998	38.9
30/10/1998 18:00	14.9	-86.5	45	998	38.9
30/10/1998 21:00	14.8	-86.7	45	999	38.9
31/10/1998 00:00	14.7	-87.0	45	999	38.9
31/10/1998 03:00	14.6	-87.3	43	1000	39.4
31/10/1998 06:00	14.5	-87.7	40	1000	40.1
31/10/1998 09:00	14.5	-88.1	38	1000	40.6

31/10/1998 12:00	14.5	-88.5	35	1000	41.3
31/10/1998 15:00	14.5	-88.8	33	1001	41.8
31/10/1998 18:00	14.6	-89.2	30	1001	42.5
31/10/1998 21:00	14.6	-89.6	30	1002	42.5
01/11/1998 00:00	14.6	-90.0	30	1002	42.5
01/11/1998 03:00	14.6	-90.4	28	1003	43.0
01/11/1998 06:00	14.7	-90.8	25	1003	43.7
01/11/1998 09:00	14.8	-91.2	25	1004	43.7
01/11/1998 12:00	14.9	-91.5	25	1005	43.7
01/11/1998 15:00	15.2	-91.9	25	1005	43.7
01/11/1998 18:00	15.5	-92.2	25	1005	43.7
01/11/1998 21:00	15.9	-92.5	23	1005	44.2
02/11/1998 00:00	16.3	-92.7	20	1005	44.9
02/11/1998 03:00	16.7	-92.9	20	1005	44.9
02/11/1998 06:00	17.1	-93.1	20	1005	44.9
02/11/1998 09:00	17.5	-93.3	20	1005	44.9
02/11/1998 12:00	17.9	-93.4	20	1005	44.9
02/11/1998 15:00	18.3	-93.6	20	1005	44.9
02/11/1998 18:00	18.7	-93.7	20	1005	44.9
02/11/1998 21:00	19.0	-93.6	20	1004	44.9
03/11/1998 00:00	19.2	-93.4	20	1003	44.9
03/11/1998 03:00	19.3	-93.1	20	1003	44.9
03/11/1998 06:00	19.3	-92.7	20	1003	44.9
03/11/1998 09:00	19.3	-92.4	23	1003	44.2
03/11/1998 12:00	19.4	-92.1	25	1002	43.7
03/11/1998 15:00	19.5	-91.8	33	1000	41.8
03/11/1998 18:00	19.6	-91.4	40	997	40.1
03/11/1998 21:00	19.8	-90.9	38	997	40.6
04/11/1998 00:00	20.0	-90.6	35	997	41.3
04/11/1998 02:00	20.1	-90.5	35	998	41.3
04/11/1998 03:00	20.2	-90.3	34	998	41.5
04/11/1998 06:00	20.8	-89.6	30	998	42.5
04/11/1998 09:00	21.3	-88.9	35	998	41.3
04/11/1998 12:00	21.8	-88.2	40	998	40.1
04/11/1998 15:00	22.5	-87.4	40	996	40.1
04/11/1998 18:00	23.3	-86.5	40	993	40.1
04/11/1998 21:00	24.1	-85.7	43	993	39.4
05/11/1998 00:00	24.8	-84.8	45	993	38.9
05/11/1998 03:00	25.3	-83.9	48	992	38.2
05/11/1998 06:00	25.6	-83.1	50	990	37.7
05/11/1998 09:00	25.8	-82.6	53	989	37.0
05/11/1998 11:00	26.2	-81.9	55	989	36.5
05/11/1998 12:00	26.6	-81.3	55	987	36.5
05/11/1998 15:00	27.2	-79.7	53	990	37.0
05/11/1998 18:00	27.5	-78.3	50	992	37.7
05/11/1998 21:00	28.6	-76.7	50	993	37.7
06/11/1998 00:00	30.0	-75.0	50	993	37.7
06/11/1998 03:00	31.2	-73.5	50	993	37.7
06/11/1998 06:00	32.5	-72.0	50	992	37.7
06/11/1998 09:00	33.8	-70.1	50	991	37.7
06/11/1998 12:00	35.0	-68.0	50	990	37.7
06/11/1998 15:00	36.0	-65.6	50	990	37.7
06/11/1998 18:00	37.0	-63.0	50	989	37.7
06/11/1998 21:00	38.0	-60.5	50	990	37.7
07/11/1998 00:00	39.0	-58.0	50	990	37.7
07/11/1998 03:00	40.0	-55.5	50	991	37.7
07/11/1998 06:00	41.0	-53.0	50	992	37.7
07/11/1998 09:00	41.7	-50.3	50	989	37.7
07/11/1998 12:00	42.5	-47.5	50	986	37.7

07/11/1998 15:00	43.5	-44.7	55	979	36.5
07/11/1998 18:00	44.5	-42.0	60	972	35.3
07/11/1998 21:00	45.5	-39.2	60	973	35.3
08/11/1998 00:00	46.5	-36.5	60	974	35.3
08/11/1998 03:00	47.5	-33.8	60	973	35.3
08/11/1998 06:00	48.5	-31.0	60	972	35.3
08/11/1998 09:00	49.1	-27.9	60	967	35.3
08/11/1998 12:00	50.0	-25.0	60	962	35.3
08/11/1998 15:00	51.7	-22.8	60	959	35.3
08/11/1998 18:00	53.5	-20.5	60	956	35.3
08/11/1998 21:00	54.6	-17.4	60	956	35.3
09/11/1998 00:00	55.5	-14.5	60	956	35.3
09/11/1998 03:00	56.7	-12.1	60	956	35.3
09/11/1998 06:00	58.0	-10.5	60	956	35.3
09/11/1998 09:00	59.5	-10.3	60	956	35.3
09/11/1998 12:00	61.0	-10.0	60	956	35.3
09/11/1998 15:00	62.3	-8.1	58	958	35.8
09/11/1998 18:00	63.5	-5.0	55	960	36.5

WIND AND PRESSURE FIELDS GENERATION

The MIKE21 Cyclone Wind Generation Tool of DHI [26] was used to generate the cyclonic wind and pressure fields for the passage of Hurricane Mitch. The tool allows users to compute wind and pressure data due to tropical cyclones. Several cyclone parametric models are included in the tool such as Young and Sobey model (1981) [29], Holland – single vortex model (1981), Holland – double vortex model (1980) [30] and Rankine vortex model. The Young and Sobey model (1981) [29] were used in the study. The Young and Sobey model (1981) [29] require six input parameters (i.e., time, track, radius of maximum wind speed, maximum wind speed, central pressure, and neutral pressure). The other models require some additional parameters (such as Holland parameter B and Rankine parameter X) that need to be calculated using empirical relationships. This adds further uncertainty to the generated wind and pressure fields. Therefore, the other models were not used for this study.

Radius of maximum wind speed was not available in the IBTrACS dataset and was, therefore, estimated using Quiring et al. [25].

It should be noted that the 1-minute mean wind speeds in Table 9 were converted into 1-hour mean using the methodology described in the World Meteorological Organisation (WMO) [31] for use in the Cyclone Wind Generation Tool. Usually, 1-hour mean wind speeds are used for numerical modelling of cyclone waves and surge.

According to Young and Sobey (1981) [29], the rotational wind gradient speed Vg at a distance r from the centre of the cyclone is given by:

$$V_g(r) = V_{max} \cdot \left(\frac{r}{R_{mw}}\right)^7 . exp\left(7\left(1 - \frac{r}{R_{mw}}\right)\right) \qquad \text{for } r < R_{mw}$$

$$V_g(r) = V_{max} . exp\left((0.0025R_{mw} + 0.05)\left(1 - \frac{r}{R_{mw}}\right)\right) \qquad \text{for } r \geq R_{mw}$$

Where, Rmw is the radius to maximum wind speed and Vmax is the maximum wind speed.

Following the Shore Protection Manual (1984) [32], the pressure p is given by:

$$p(r) = p_c + (p_n - p_c). exp\left(-\frac{R_{mw}}{r}\right)$$

Where, pc is the pressure at the storm centre (or central pressure) and pn is the ambient surroundings pressure field (or neutral pressure).

Three types of wind corrections are available in the Cyclone Wind Generation Tool of DHI [26] to reflect the cyclonic wind structure. These wind corrections are described below from the Scientific Documentation of the Cyclone Wind Generation Tool of DHI [26].

a) Geostrophic Correction

The parametric models usually provide wind information at the geo¬strophic or gradient wind level above the influence of the planetary boundary layer. This gradient wind speed (V_g) may be reduced to the standard surface reference level (V_{10}) by considering the effects of the boundary layers as below:

$$V_{10}(r) = K_m . V_g(r)$$

Where, $V_g(r)$ is the rotational gradient wind speed (m/s) at a distance r from the centre of the cyclone, V10 is the near-surface wind speed (m/s), and K_m is the boundary layer wind speed correction coefficient.
Three options are available in the DHI tool [26], namely no correction, constant correction, and Harper et al. (2001) [33]. Harper et al. (2001) [33] empirical formulation was used in the present study where Km is dependent on Vg through a set of equa¬tions as below:

$$K_m = \begin{cases} 0.81 & for\ V_g < 6\ m/s \\ 0.81 - 2.96\ 10^{-3}(V_g - 6) & for\ 6 \le V_g < 19.5 \\ 0.77 - 4.31\ 10^{-3}(V_g - 19.5) & for\ 19.5 \le V_g < 45 \\ 0.66 & for\ V_g > 45\ m/s \end{cases}$$

b) Forward Motion Asymmetry
Cyclone winds circulate clockwise in the Southern Hemisphere and anticlockwise in the Northern Hemisphere. The wind field is asymmetric so that winds are typically stronger to the left of cyclone's track and lower to the right due to the contribution of the cyclone movement.
Two options are available in the DHI tool to consider the forward motion asymmetry at surface level, namely no correction and Harper et al. (2001) [33]. Harper et al. (2001) [33] empirical formulation (as below) was used in the present study where the user must specify the proportion of the cor¬rection factor, delta (δ_{fm}) and the angle of maximum winds, theta max (θ_{max}). The proportion of the added forward cyclone speed (V_{fm}) can be adjusted using the correction factor delta (δ_{fm}). Theta max (θ_{max}) is measured relative to the cyclone movement direction. In the DHI tool, the cyclone movement direction and the cyclone speed are computed based on the position of the centre of the storm given in the best track data table.

$$V_{10}(r,\theta) = K_m . V_g(r) + \delta_{fm}.V_{fm}.cos(\theta_{max} - \theta)$$

c) Inflow Angle
All the parametric wind models described earlier assume a circular wind flow pattern which does not represent the observed surface wind directions. Friction effects between water and air cause a deflection of the wind direction towards the centre of the cyclone. Two options are available in the DHI tool, namely no correction and Sobey et al. (1977) [34]. Sobey et al. (1977) [34] empirical formulation (as below) was used in the present study where the deflection is characterised by the inflow angle (β) in the order of 25° but decreases towards the storm centre.

$$\beta = \begin{cases} 10 \dfrac{r}{R_{mw}} & \text{for}\ \ 0 \le r < R_{mw} \\ 10 + 75\left(\dfrac{r}{R_{mw}} - 1\right) & \text{for}\ \ R_{mw} \le r < 1.2\, R_{mw} \\ 25 & \text{for}\ \ r \ge 1.2\, R_{mw} \end{cases}$$

RESULTS AND DISCUSSIONS

Two-dimensional wind and pressure fields were generated along the entire path of Hurricane Mitch. Then two-dimensional wind and pressure fields at key selected locations were extracted. The selected locations are shown in Figure 4. Coordinates, hourly timesteps and date and time of these locations are provided in Table 10.

Figure 4: Wind and pressure fields extraction locations

Table 10: Wind and pressure fields extraction locations, timesteps and date and time

Locations	Coordinates		Date and time	Hourly timesteps
	Latitude (°N)	Longitude (°W)		
P1	11.6	-76.1	22/10/1998 00:00	0
P2	11.8	-77.6	23/10/1998 00:00	24
P3	13.4	-77.9	24/10/1998 00:00	48
P4	15.5	-78.4	25/10/1998 00:00	72
P5	16.4	-81.0	26/10/1998 00:00	96
P6	17.2	-83.8	27/10/1998 00:00	120
P7	16.6	-85.6	28/10/1998 00:00	144
P8	16.3	-85.6	28/10/1998 12:00	156
P9	16.2	-85.8	29/10/1998 00:00	168
P16	20.0	-90.6	04/11/1998 00:00	312
P17	24.1	-85.7	04/11/1998 21:00	336
P18	25.8	-82.6	05/11/1998 09:00	348
P19	27.5	-78.3	05/11/1998 18:00	360

The top plot in Figures 5 to 17 show the two-dimensional wind fields when the hurricane reached to the selected locations (P1 to P9, P16 to P17) respectively. The time-series of wind speeds at these locations during the entire passage of the hurricane are presented at the bottom of these figures. Figure 18 compares the time-series of wind speeds at the selected locations during the entire passage of the hurricane.

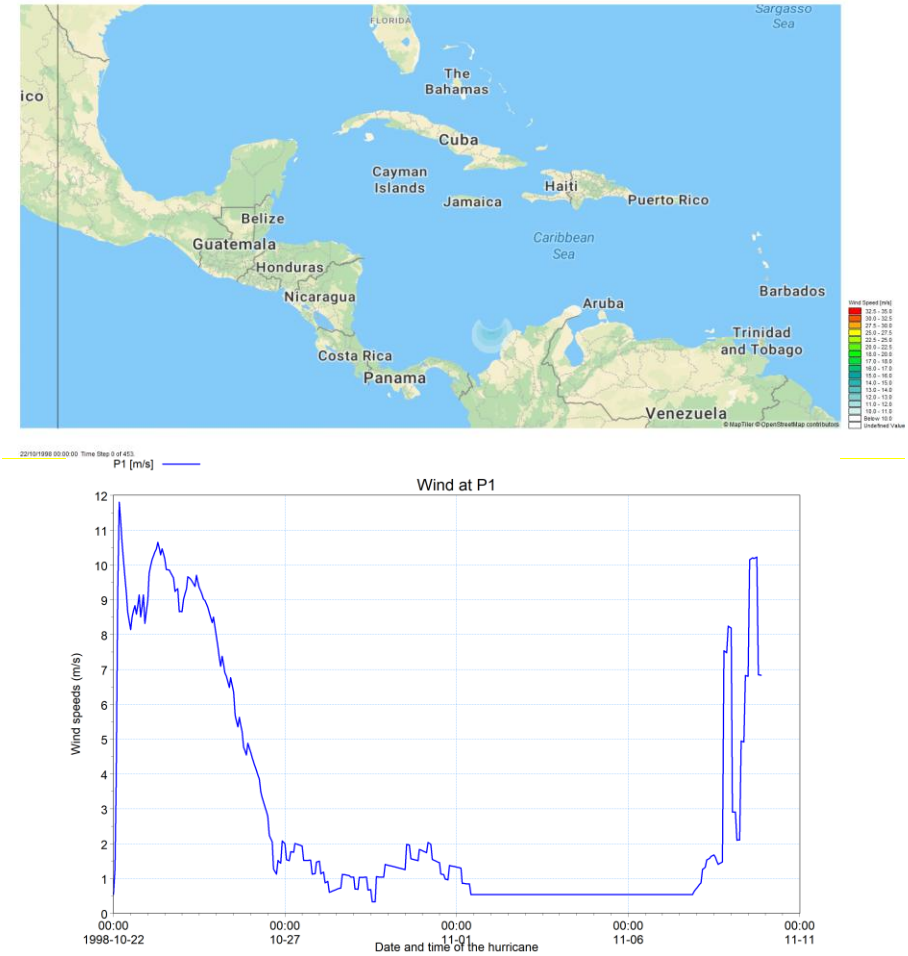

Figure 5: Wind field of Hurricane Mitch at P1 (top – 2D wind field; bottom – time-series of wind speeds)

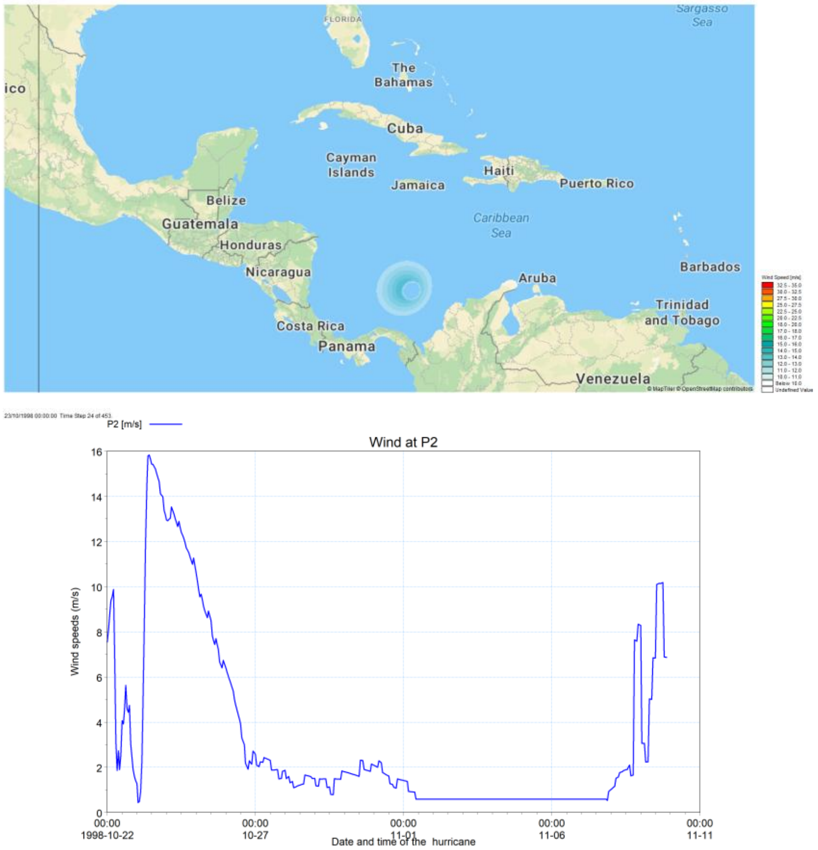

Figure 6: Wind field of Hurricane Mitch at P2 (top – 2D wind field; bottom – time-series of wind speeds)

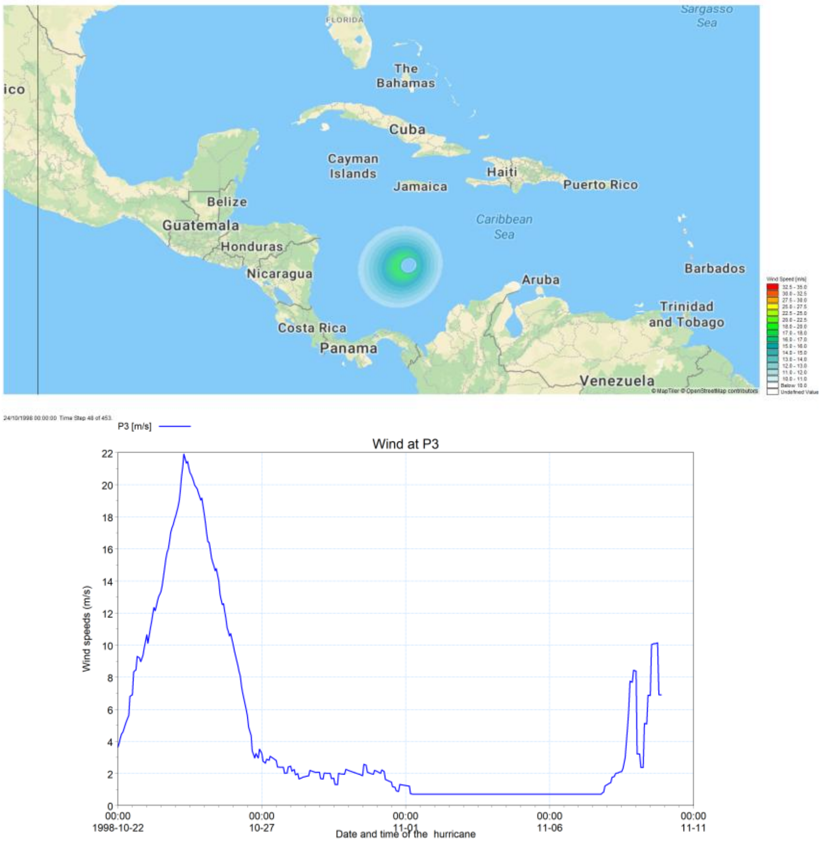

Figure 7: Wind field of Hurricane Mitch at P3 (top – 2D wind field; bottom – time-series of wind speeds)

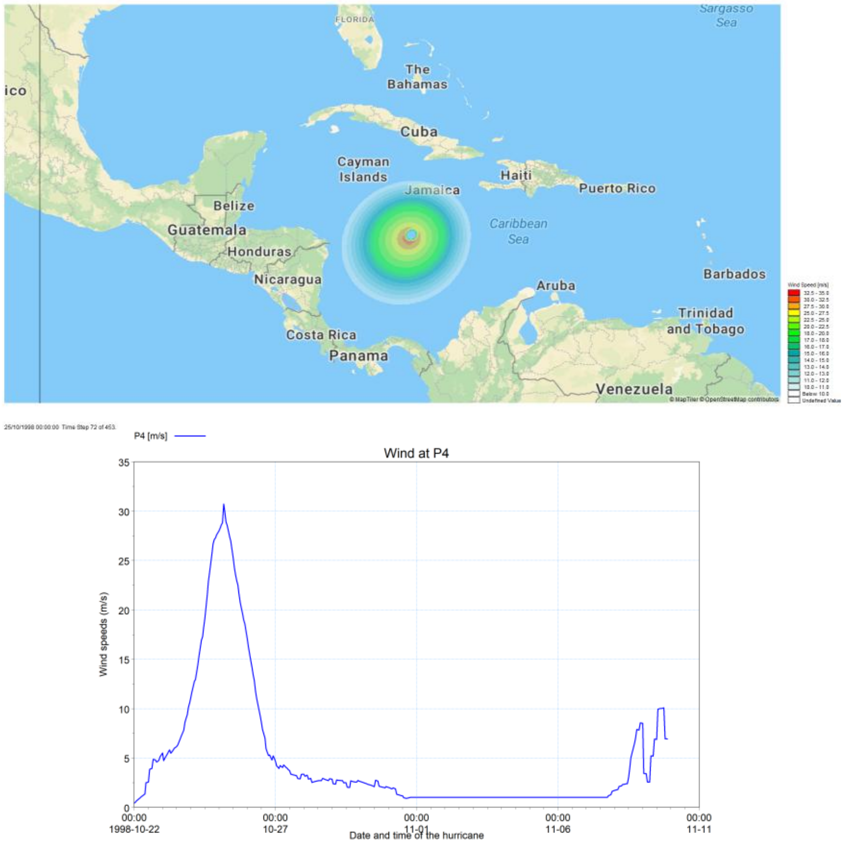

Figure 8: Wind field of Hurricane Mitch at P4 (top – 2D wind field; bottom – time-series of wind speeds)

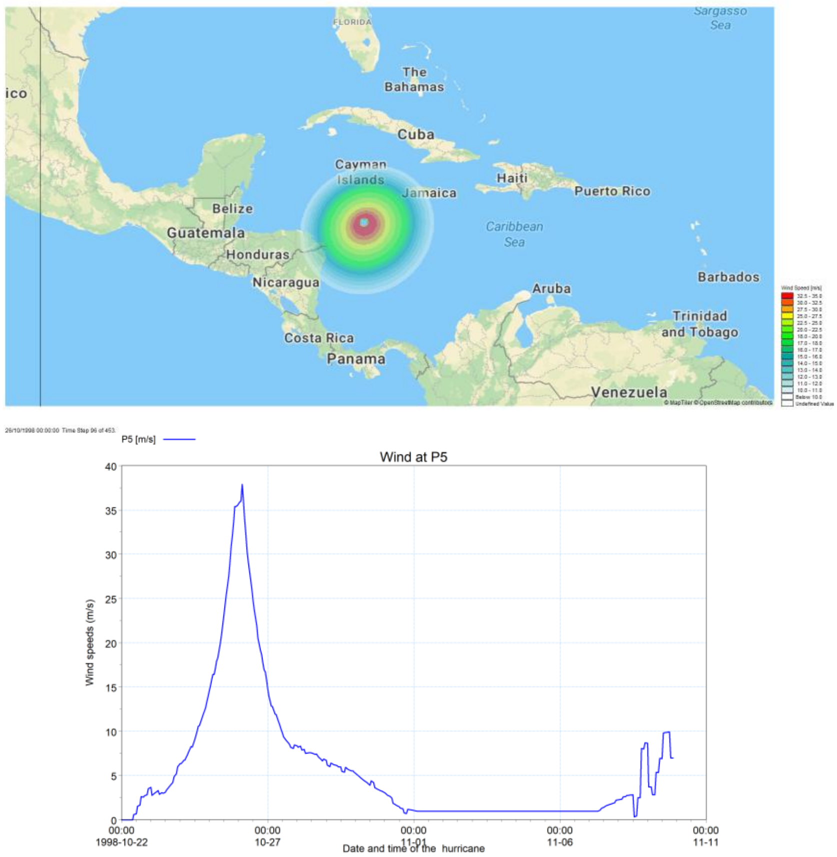

Figure 9: Wind field of Hurricane Mitch at P5 (top – 2D wind field; bottom – time-series of wind speeds)

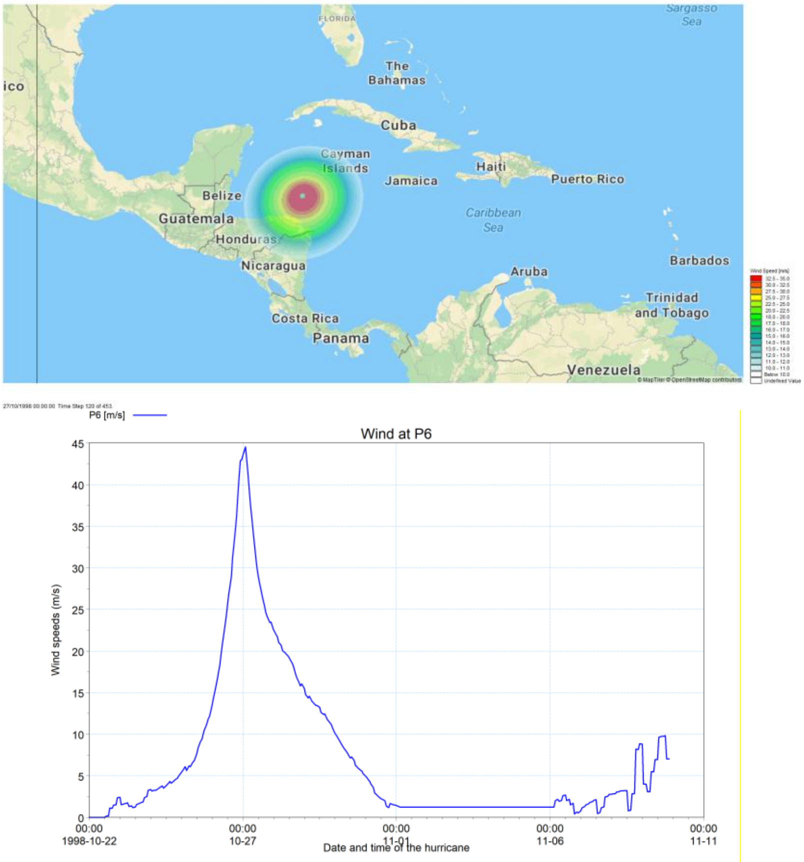

Figure 10: Wind field of Hurricane Mitch at P6 (top – 2D wind field; bottom – time-series of wind speeds)

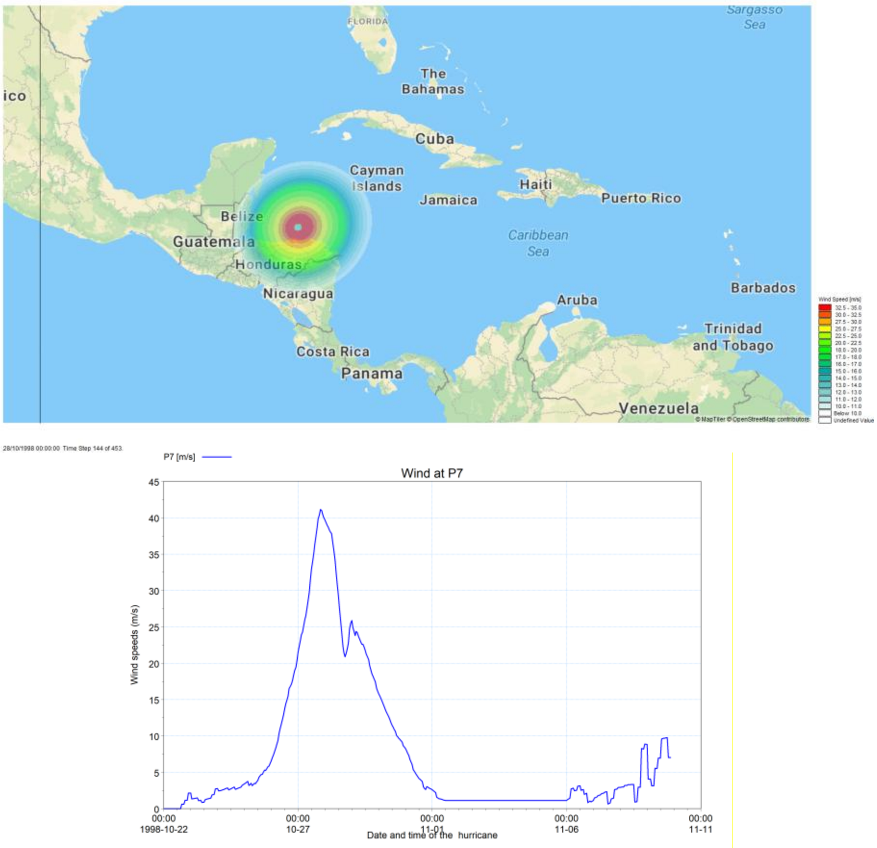

Figure 11: Wind field of Hurricane Mitch at P7 (top – 2D wind field; bottom – time-series of wind speeds)

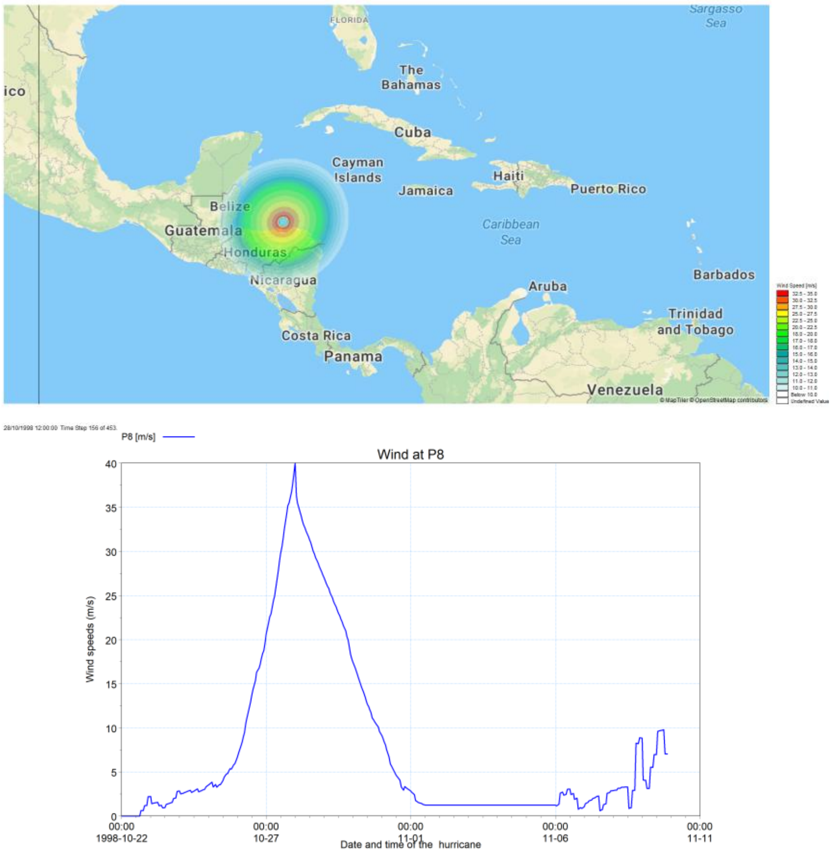

Figure 12: Wind field of Hurricane Mitch at P8 (top – 2D wind field; bottom – time-series of wind speeds)

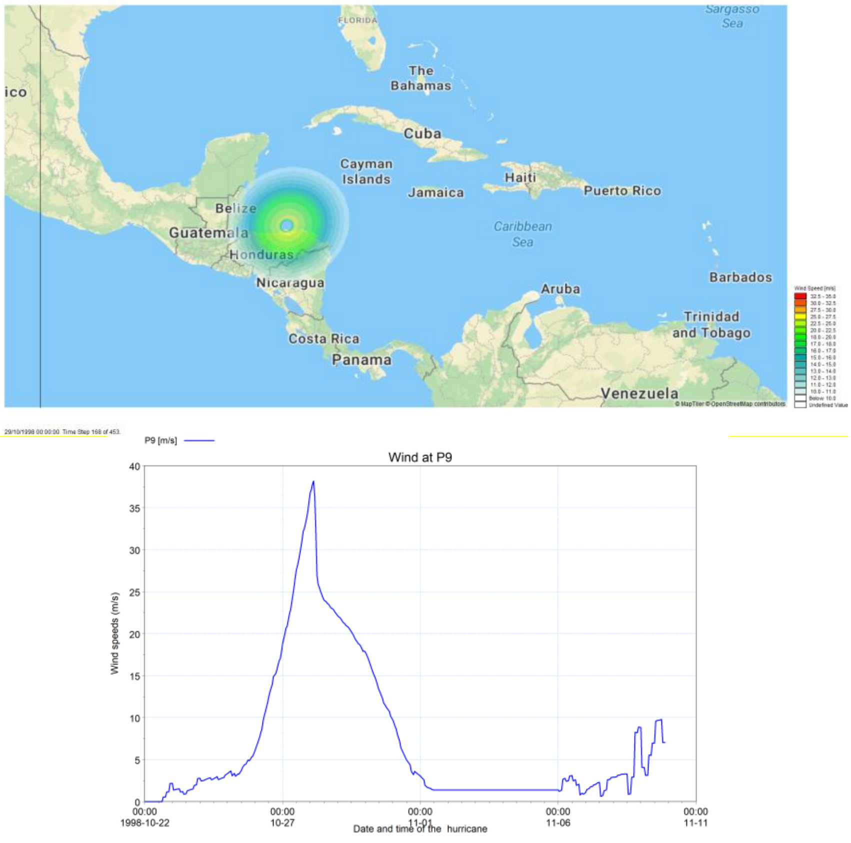

Figure 13: Wind field of Hurricane Mitch at P9 (top – 2D wind field; bottom – time-series of wind speeds)

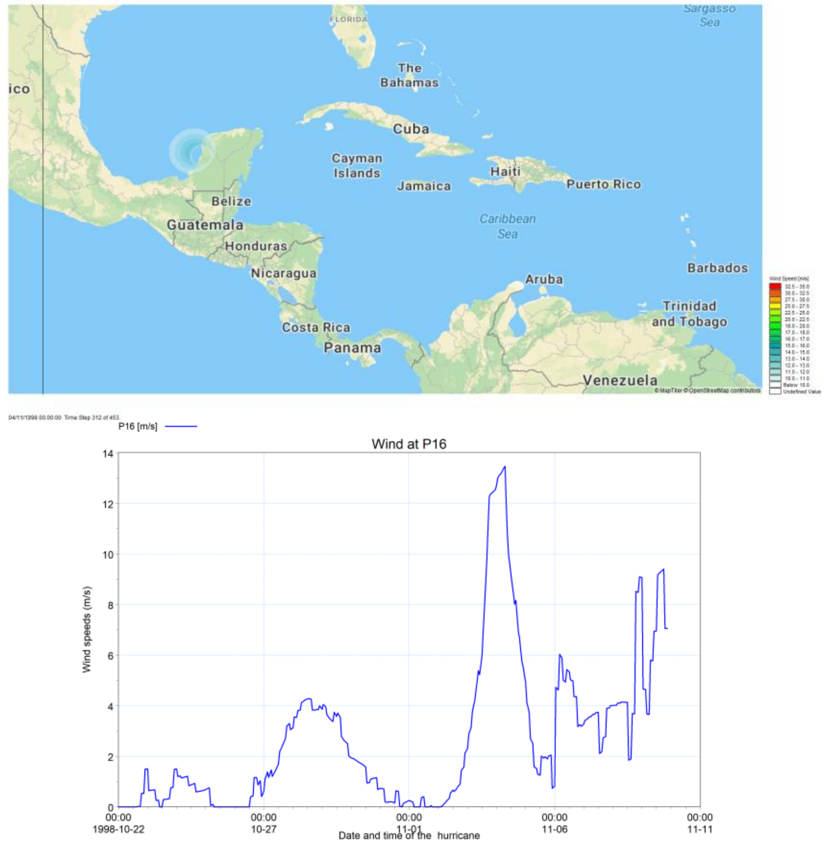

Figure 14: Wind field of Hurricane Mitch at P16 (top – 2D wind field; bottom – time-series of wind speeds)

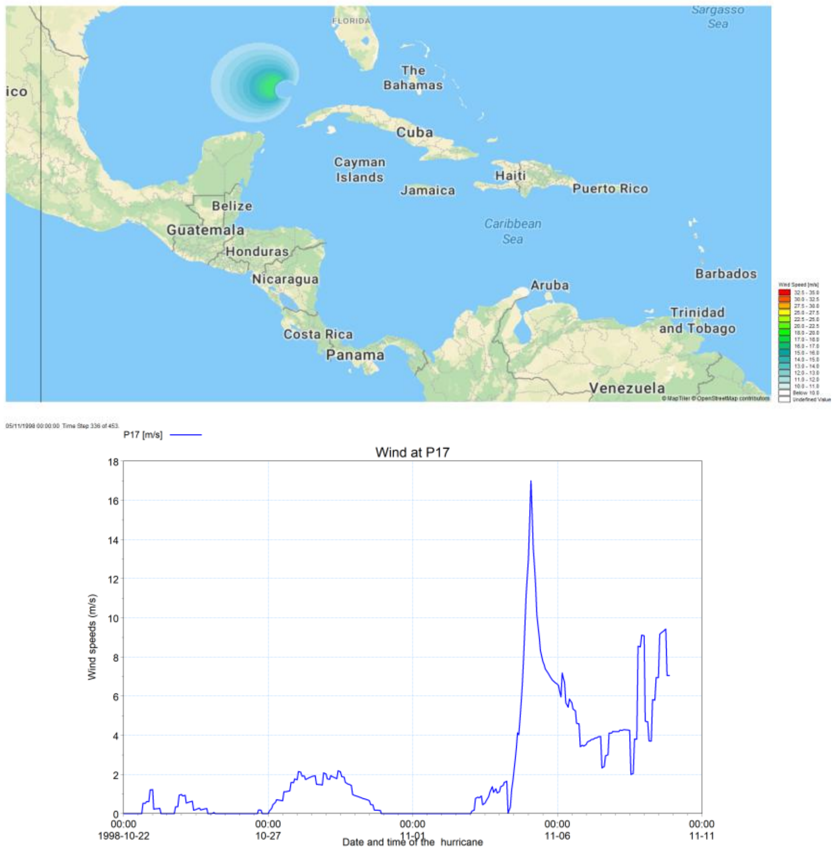

Figure 15: Wind field of Hurricane Mitch at P17 (top – 2D wind field; bottom – time-series of wind speeds)

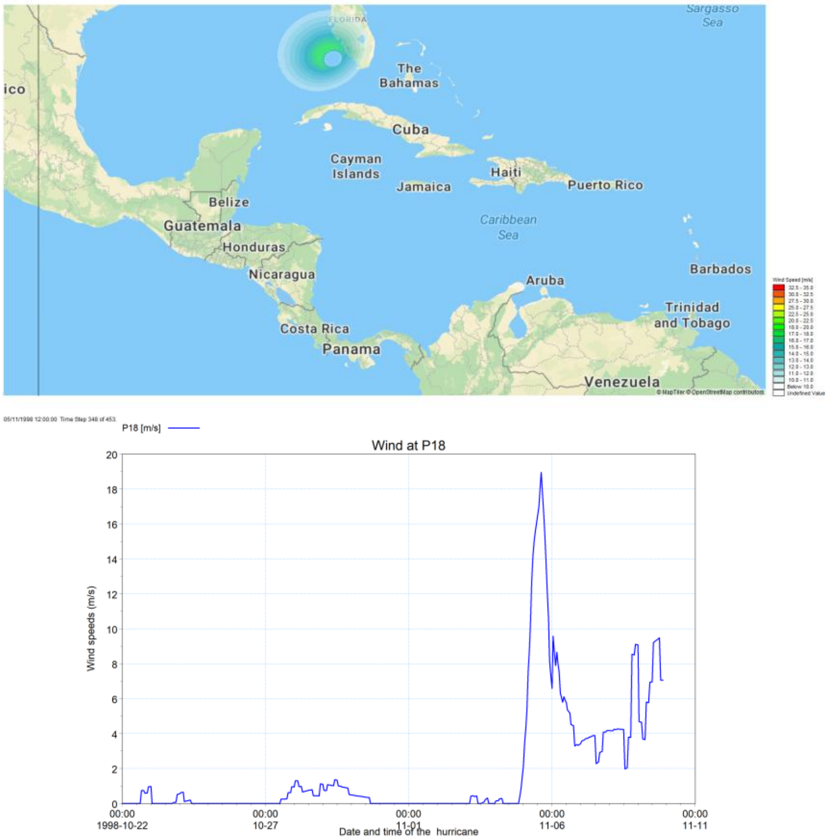

Figure 16: Wind field of Hurricane Mitch at P18 (top – 2D wind field; bottom – time-series of wind speeds)

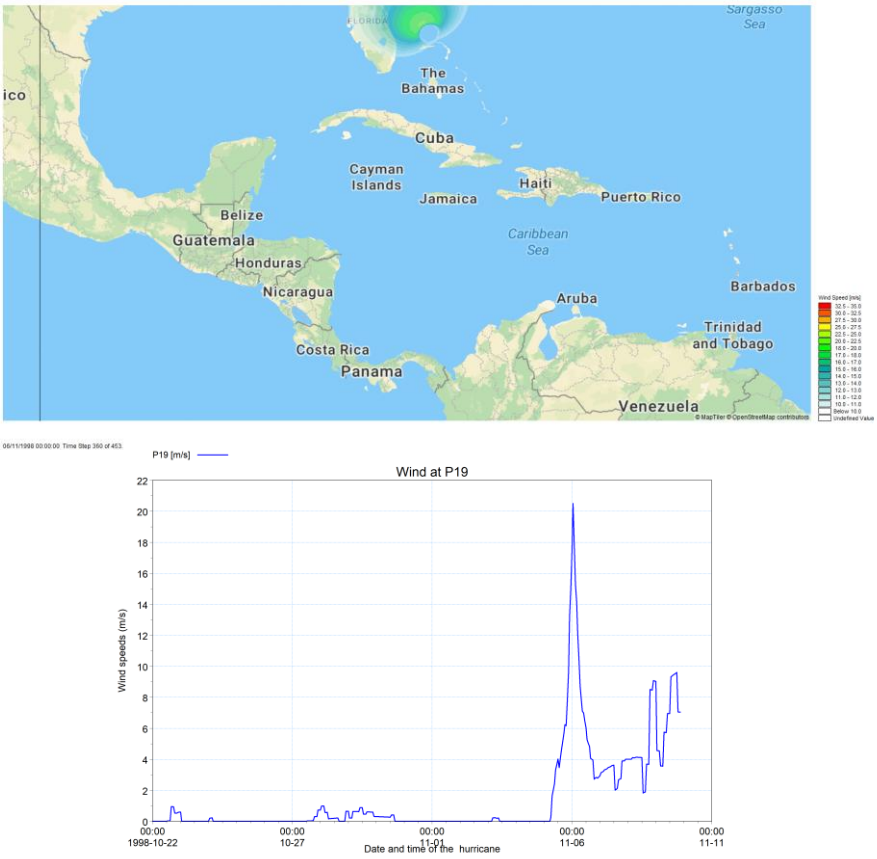

Figure 17: Wind field of Hurricane Mitch at P19 (top – 2D wind field; bottom – time-series of wind speeds)

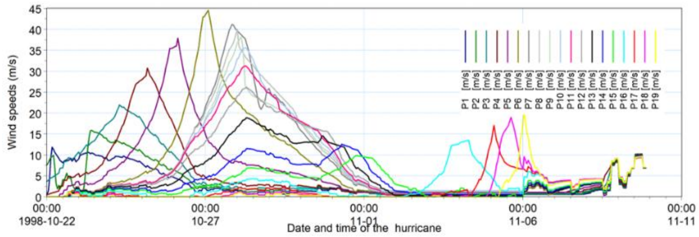

Figure 18: Time-series of hourly-mean wind speeds at the selected locations during the entire passage of Hurricane Mitch

Figure 19: Pressure field of Hurricane Mitch at P1 (top – 2D pressure field; bottom – time-series of pressure)

Figure 20: Pressure field of Hurricane Mitch at P2 (top – 2D pressure field; bottom – time-series of pressure)

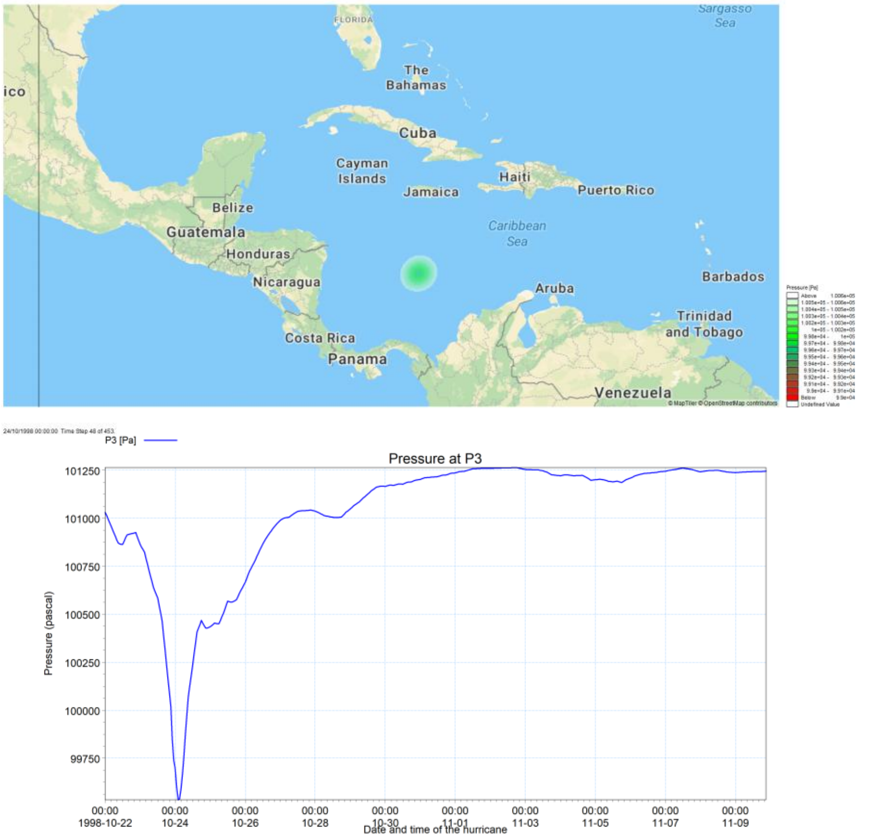

Figure 21: Pressure field of Hurricane Mitch at P3 (top – 2D pressure field; bottom – time-series of pressure)

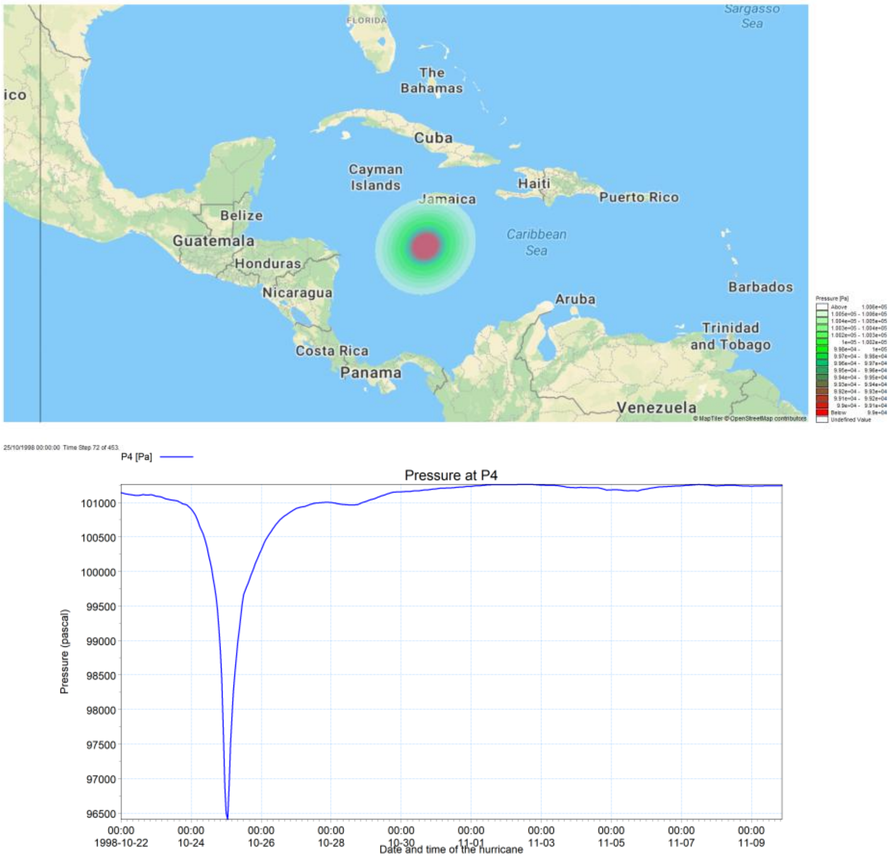

Figure 22: Pressure field of Hurricane Mitch at P4 (top – 2D pressure field; bottom – time-series of pressure)

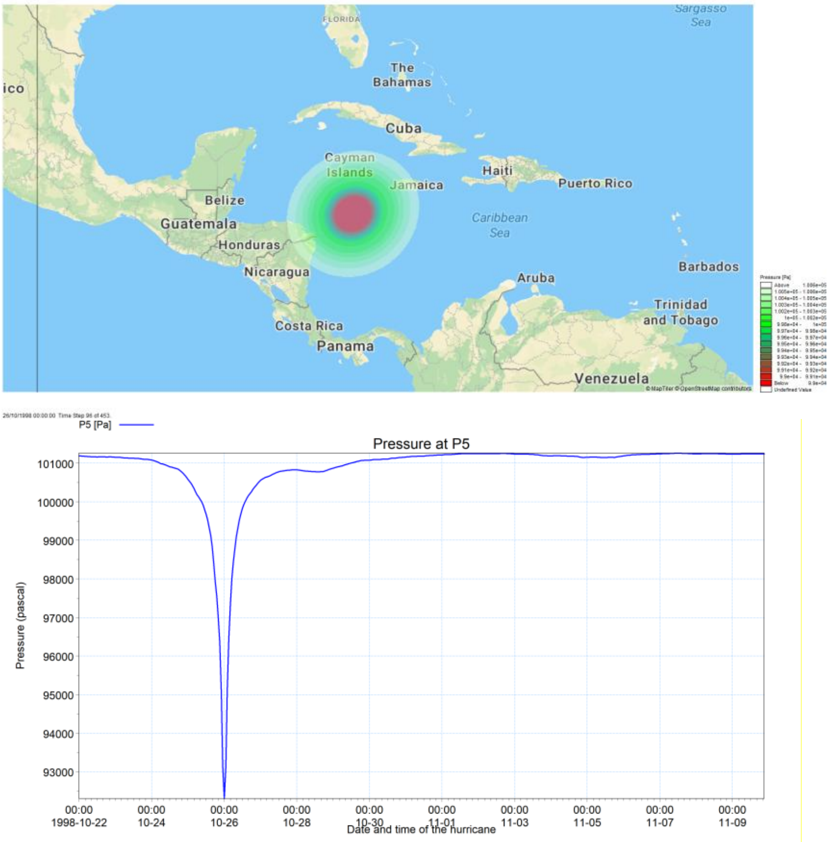

Figure 23: Pressure field of Hurricane Mitch at P5 (top – 2D pressure field; bottom – time-series of pressure)

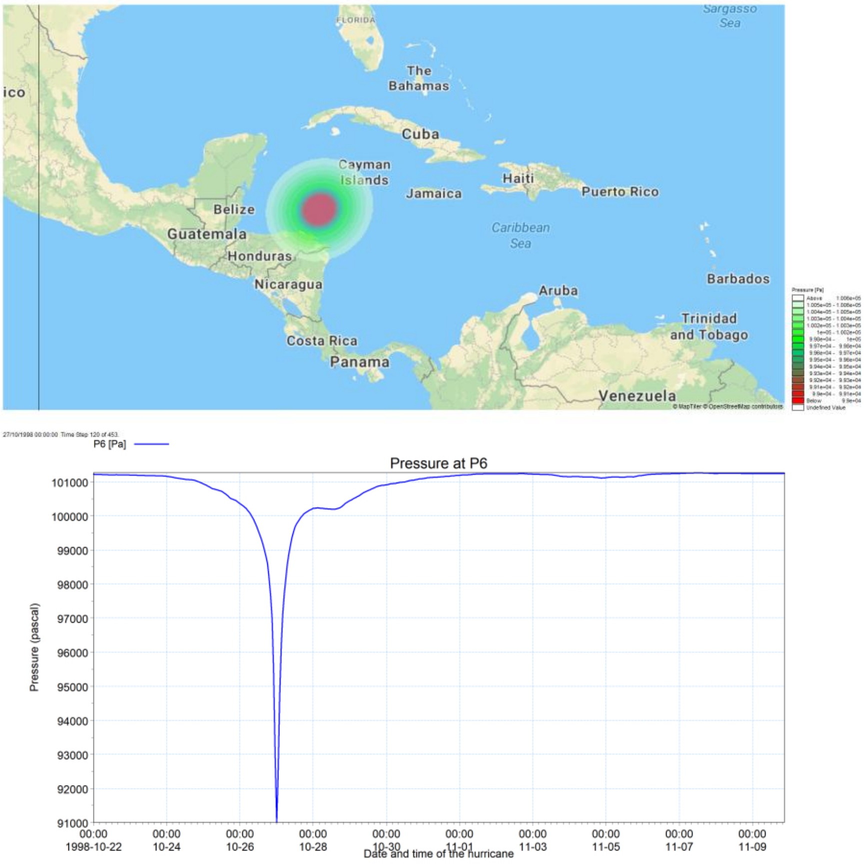

Figure 24: Pressure field of Hurricane Mitch at P6 (top – 2D pressure field; bottom – time-series of pressure)

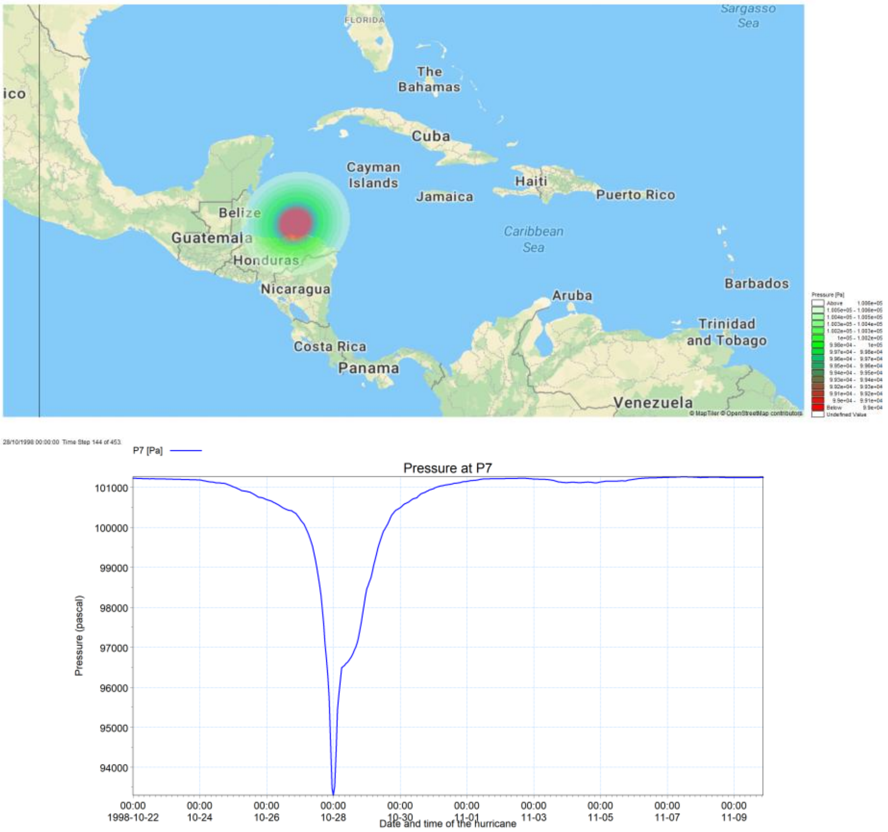

Figure 25: Pressure field of Hurricane Mitch at P7 (top – 2D pressure field; bottom – time-series of pressure)

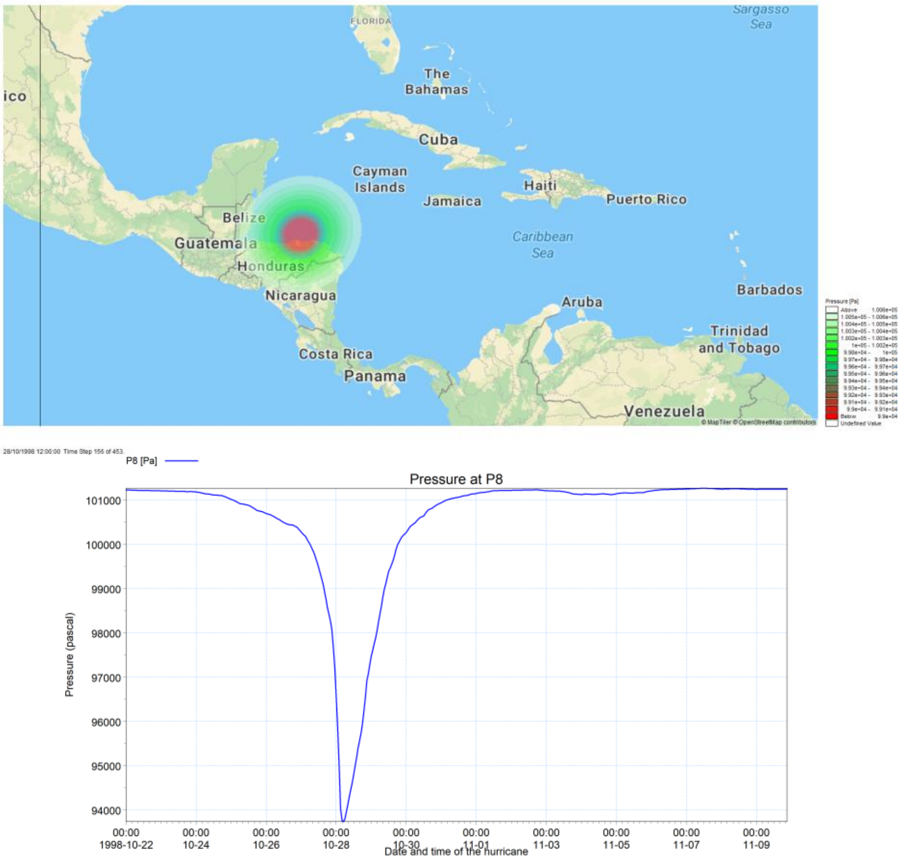

Figure 26: Pressure field of Hurricane Mitch at P8 (top – 2D pressure field; bottom – time-series of pressure)

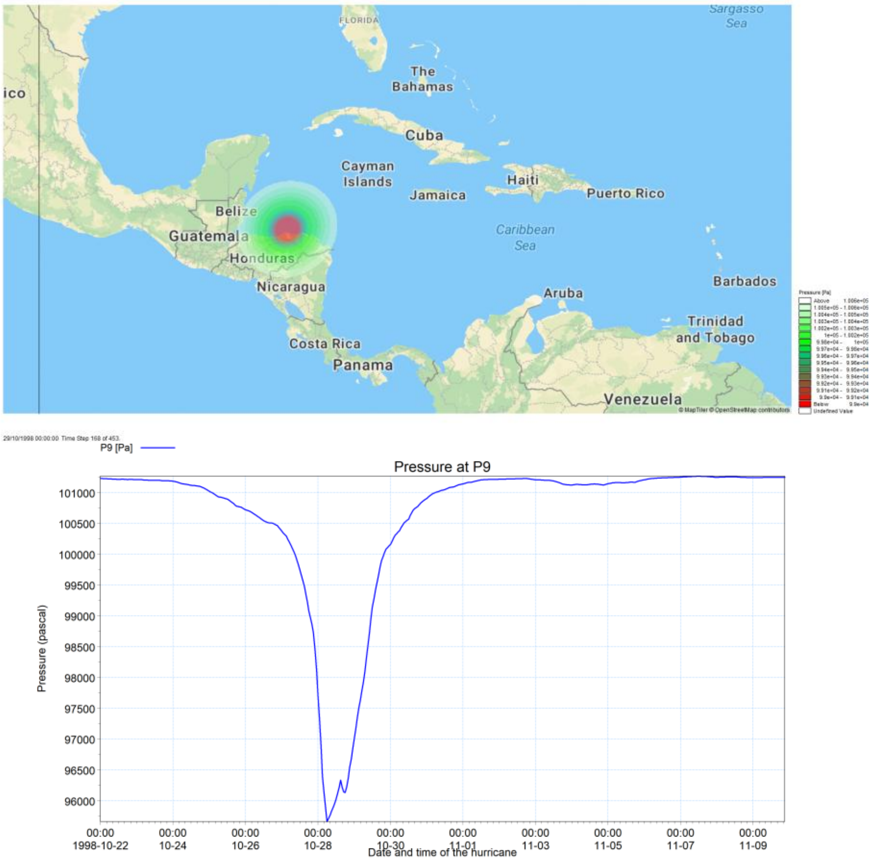

Figure 27: Pressure field of Hurricane Mitch at P9 (top – 2D pressure field; bottom – time-series of pressure)

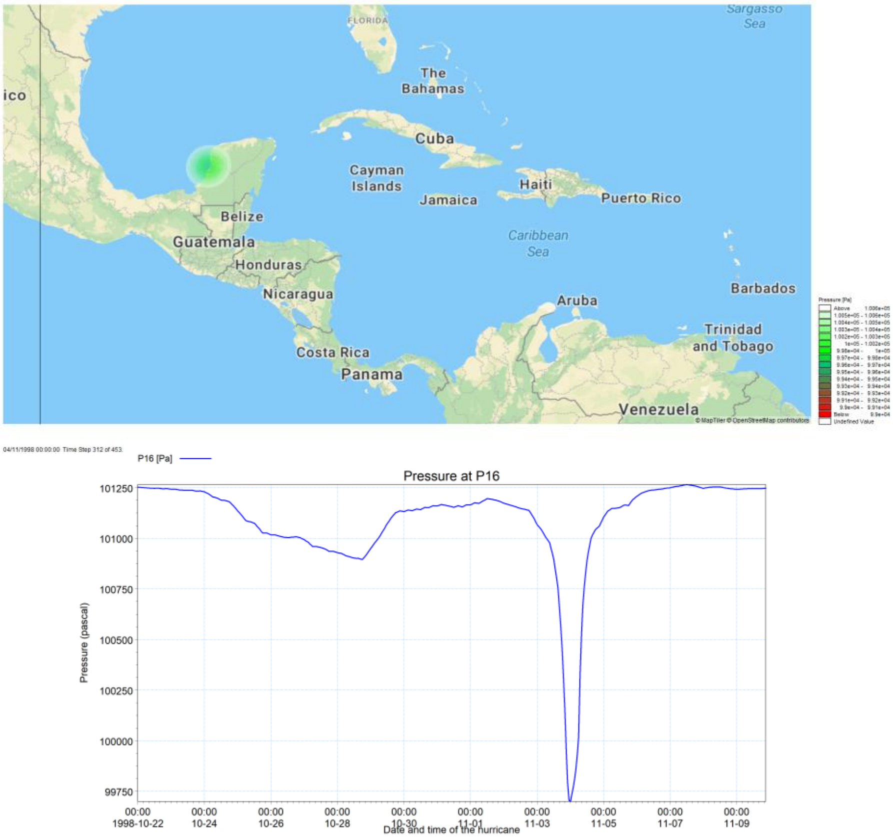

Figure 28: Pressure field of Hurricane Mitch at P16 (top – 2D pressure field; bottom – time-series of pressure)

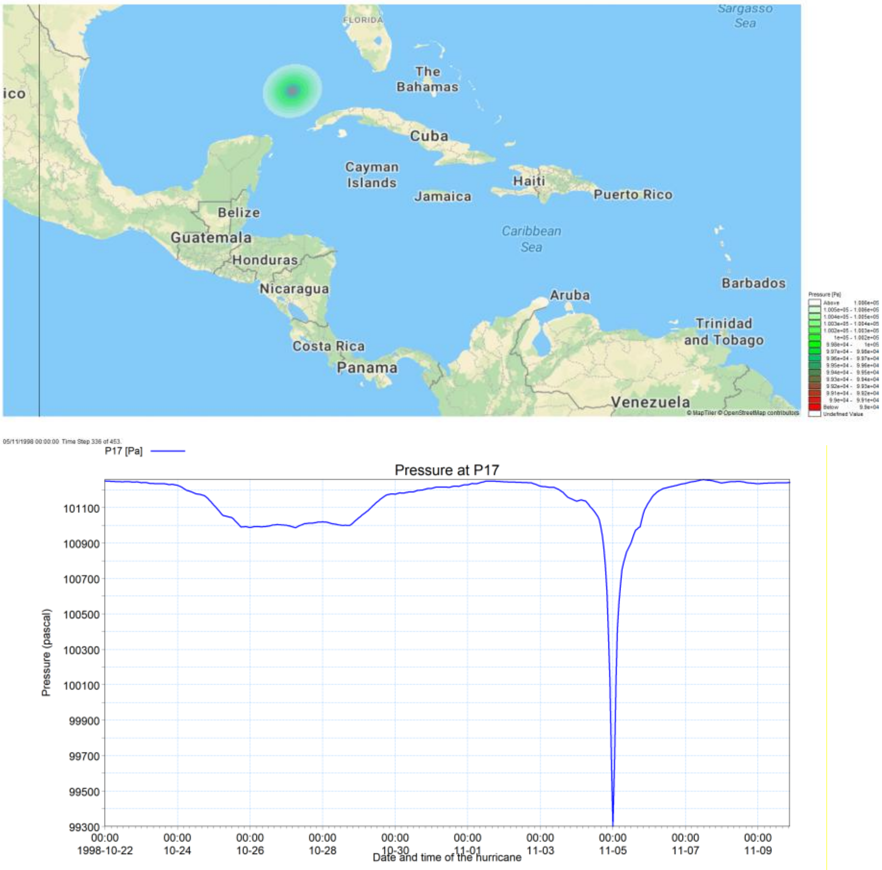

Figure 29: Pressure field of Hurricane Mitch at P17 (top – 2D pressure field; bottom – time-series of pressure)

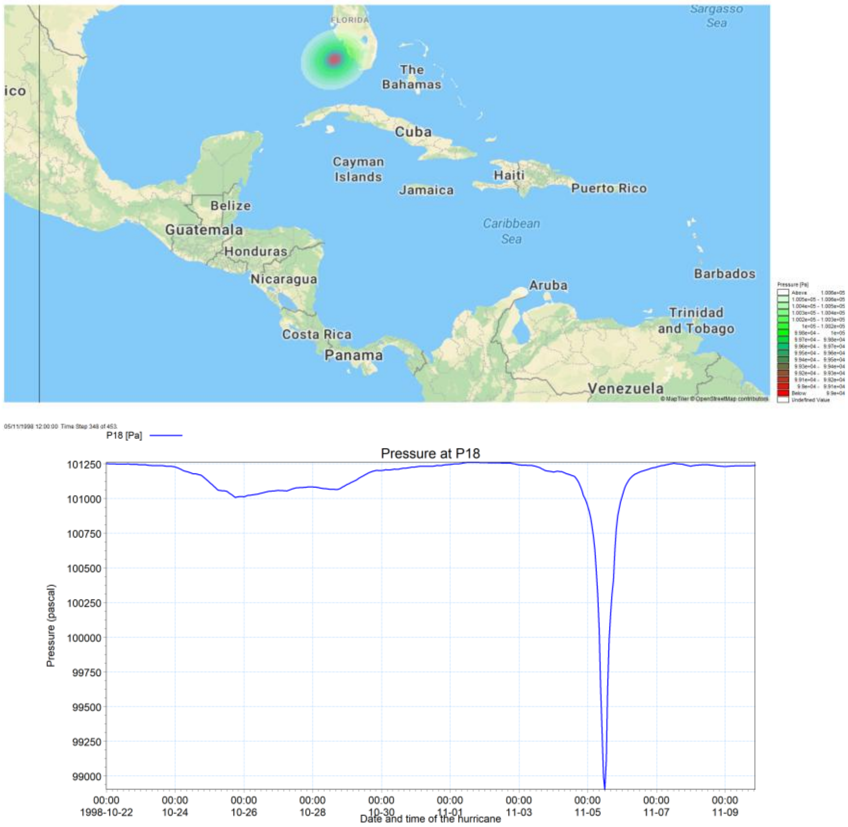

Figure 30: Pressure field of Hurricane Mitch at P18 (top – 2D pressure field; bottom – time-series of pressure)

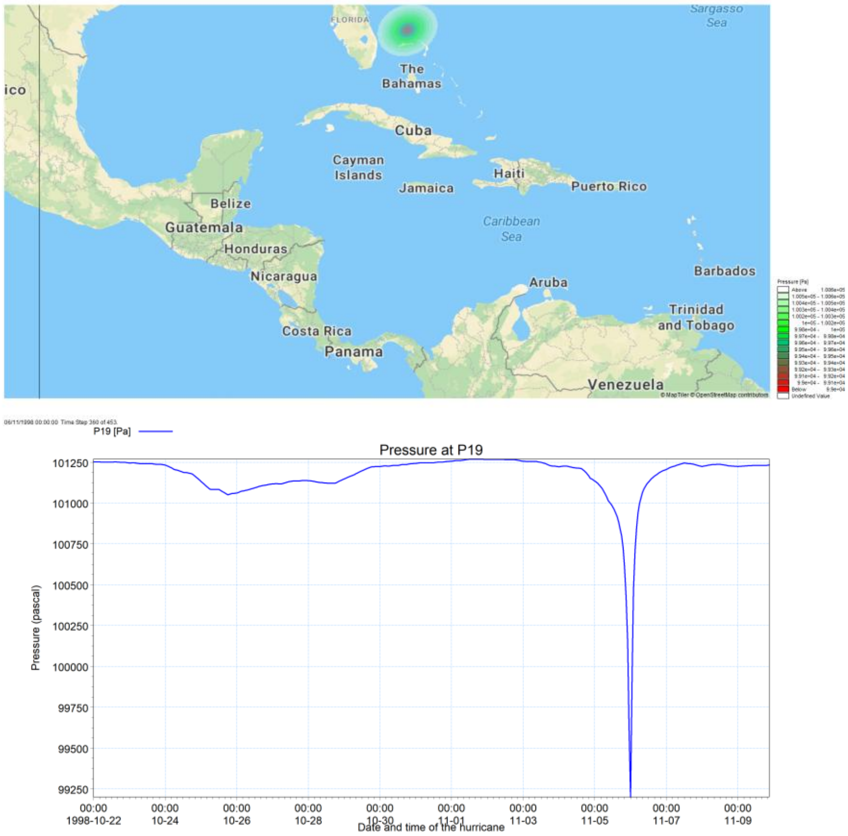

Figure 31: Pressure field of Hurricane Mitch at P19 (top – 2D pressure field; bottom – time-series of pressure)

The top plot in Figures 19 to 31 show the two-dimensional pressure fields when the hurricane reached to the selected locations (P1 to P9, P16 to P17) respectively. The time-series of pressure at these locations during the entire passage of the hurricane are presented at the bottom of these figures. Figure 32 compares the time-series of pressure at the selected locations during the entire passage of the hurricane.

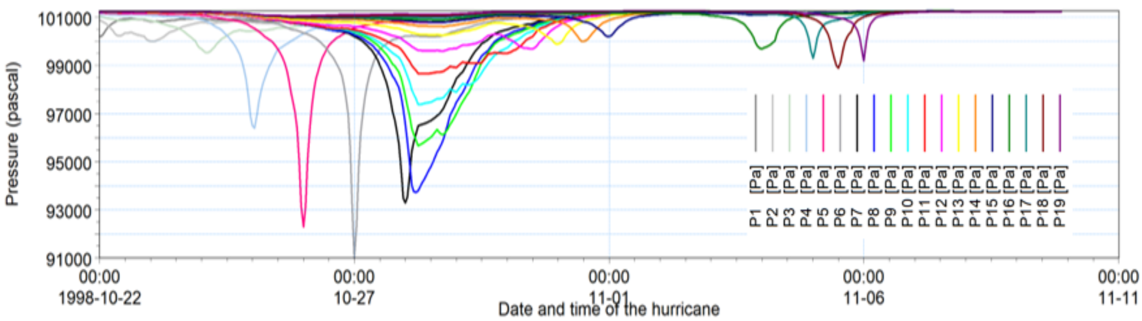

Figure 32: Time-series of pressure at the selected locations during the entire passage of Hurricane Mitch

The highest wind speeds and the lowest pressures at the selected locations during the entire passage of Hurricane Mitch are summarised in Table 11 from the time-series plots and are also shown in Figure 33. The highest wind speed and the lowest pressure are found in P6 where the hurricane reached to its peak intensity. It should be noted that 1 Hectopascal (hPa) = 100 Pascals (Pa).

Table 11: The highest wind speeds and the lowest pressures at the selected locations

Locations	Highest wind speed (m/s)	Lowest pressure (Pa)
P1	12	100,200
P2	16	100,000
P3	22	99,533
P4	31	96,407

P5	38	92,300
P6	45	91,000
P7	41	93,300
P8	40	93,734
P9	38	95,659
P16	13	99,700
P17	17	99,300
P18	19	98,900
P19	21	99,200

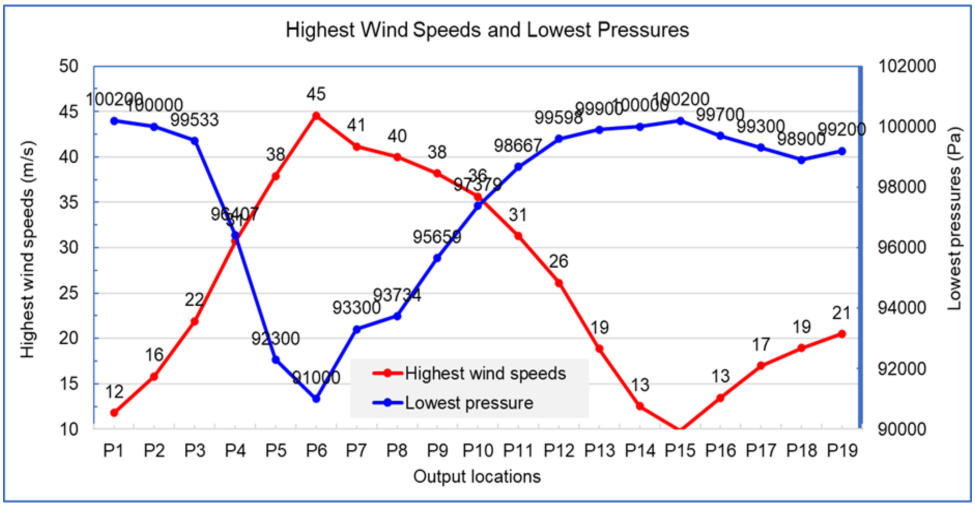

Figure 33: Highest wind speeds and lowest pressures during Hurricane Mitch at the selected locations extracted from the time-series plots

RECOMMENDED DESIGN CONSIDERATIONS

The potential impact of a cyclone event on the design of coastal and marine facilities may be summarised as follows:

1) Shoaling results in an increase in water levels and stronger currents inshore. Measures will be required to protect structures from scouring of the foreshore and seabed and limit damage to the crest if heavy overtopping occurs;
2) The foreshore will be subjected to flooding as the cyclone waves and surge approach; and
3) Facilities located on the landward slope are at risk from cyclone wave run-up and surge.

HURRICANE RISK REDUCTION MEASURES

Risks Reduction from Hurricanes

Damage due to a cyclone depends on the strength and proximity of the cyclone as well as local bathymetry and topography and the location of people, structures, and facilities. Damage due to a cyclone also depends on the landfall timing with a landfall during a high tide increases risks and damages.

It is almost impossible to fully protect people and settlements from major cyclonic events. However, various soft and hard measures (independently or in combination) could be adopted to reduce fatalities and damage to key infrastructure.

Some potential measures to reduce the risk of damage and deaths from major cyclonic events are highlighted below:

1) Detection, early warning systems and real-time observation systems are of great importance;
2) Appropriate awareness and understanding among the general public;
3) Mitigation plans and evacuation and rescue preparedness by responsible authorities;
4) Cyclone risk assessment, flood risk and inundation hazard maps;
5) Cyclone shelters;
6) Developing artificial forest such as mangroves and casuarinas of appropriate width behind the shoreline to reduce cyclone wave energy;
7) Maintaining natural sand dunes;
8) Regulations for development in the coastal zone;
9) Saline embankments to prevent salt-water entering into fertile lands;
10) Raising ground levels of important structures and facilities such as warehouses, terminals and quays; and
11) Constructing cyclone defence structures such seawalls, dykes, gates, nearshore breakwaters, and offshore barriers. However, these structures are substantial and very expensive.

For major coastal infrastructure, the adoption of appropriate design parameters, a proper assessment of structural loads, forces, and stability in combination with a detailed understanding of cyclone processes will reduce the level of damage resulting from these events. Furthermore, physical modelling of major coastal and marine structures and mooring systems to investigate their stability under severe conditions will be helpful to reduce damage due to cyclones.

Risks Reduction from Mudslides and Landslides

High tides and heavy and prolonged rains during a cyclone may cause floods and submergence of low-lying areas which may lead to mudslides and landslides in mountainous areas causing loss of life and property. Landslides and mudslides are downhill earth movements that move slowly and cause gradual damage. They can also move rapidly destroying property and taking lives suddenly and unexpectedly. They typically carry heavy debris such as trees and boulders which cause severe damage together with injury or death. Faster movement of mudslides makes them deadly.

It is not possible to prevent a mudslide or a landslide. However, preparatory steps can be taken to lessen the impact of a mudslide. Some guidelines are briefly mentioned below:

1) Carrying out risk assessment;
2) Creating public awareness and practicing an evacuation plan;
3) Staying up to date on storm/rainfall/cyclone warnings during times of increased risk;
4) Watching for any visible signs such as cracks on land, debris flows or trees tilting or boulders knocking;
5) Staying alert and awake;
6) Moving out of the path of the landslide or debris flow; and
7) Some erosion control measures might be helpful (such as installing barrier walls, improving drainage system and planting trees with deep and extensive root systems).

SUMMARY AND FINDINGS

Sufficient information on the deadliest hurricane in the Atlantic Basin (Great Hurricane, 1780) is not available to carry out numerical modelling studies whereas some information on the second deadliest tropical hurricane (Hurricane Mitch, 1998) is available. Therefore, Hurricane Mitch was selected for further studies in this paper to provide additional information.

Raw data (such as track, maximum wind speed and minimum central pressure) were obtained from IBTrACS [24]. Radius of maximum wind speed was not available in the IBTrACS dataset and was, therefore, estimated using Quiring et al. [25]. Two-dimensional wind and pressure fields along the entire track were then generated using the Cyclone Wind Generation Tool of DHI [26].

Two-dimensional wind and pressure fields at selected locations along the track of the hurricane are presented in this paper. Time-series wind speed and pressure during the entire passage of the hurricane are also provided at these selected locations.

The highest wind speeds and the lowest pressures at the selected locations are summarised both in tabular and graphical formats from the time-series plots at these locations. The highest wind speed and the lowest pressure were found at a location (P6) where the hurricane reached to its peak intensity.

The two-dimensional wind and pressure fields are useful for numerical modelling of waves and surge. Structural design considerations and cyclone risk reduction measures are also provided in this paper. The methodology described in this paper for generating wind and pressure fields from Hurricane Mitch could also be applied for other typhoons around the world.

Acknowledgements

The author would like to thank Royal HaskoningDHV (an independent, international engineering and project management consultancy company, www.royalhaskoningdhv.com) for giving permission to publish this paper. The author would like to thank his colleague Debra Griffin for carrying out the proof reading of this manuscript. The author would also like to thank the external reviewers who provided valuable comments to improve the paper.

REFERENCES

[1]. Simpson, R. H. (1974). The hurricane disaster--potential scale. Weatherwise, 27, 169. https://www.aoml.noaa.gov/general/WWW000/text/sfsimp.html.https://www.aoml.noaa.gov/hrd/Landsea/deadly/Table1.htm.

[2]. Adler, R. F. (2005). Estimating the benefit of TRMM tropical cyclone data in saving lives, June 20, 2005.

[3]. Ubydul Haque, Masahiro Hashizume, Korine N Kolivras, Hans J Overgaard, Bivash Das, and Taro Yamamotoa (2012). Reduced death rates from cyclones in Bangladesh: what more needs to be done? Bulletin of the World Health Organization, 2012 Feb 1; 90(2): 150-156, PMCID: PMC3302549, published online 2011 Oct 24. doi: 10.2471/BLT.11.088302.

[4]. Arizona State University (2020). World: Highest Mortality, Tropical Cyclone. World Meteorological Organization's World Weather & Climate Extremes Archive. Arizona State University, November 12, 2020.

[5]. Business Insider India (2017). The 16 deadliest storms of the last century, Business Insider India, September 13, 2017.

[6]. Julian, F. (2019). Remembering the great Bhola cyclone, Dhaka Tribune, November 9, 2019.

[7]. Rudolph, D. K. and Guard, C. P. (1992). 1991 Annual Tropical Cyclone Report. U.S. Naval Oceanography Command Center, Joint Typhoon Warning Center, https://web.archive.org/web/20200813232009/https://www.usno.navy.mil/NOOC/nmfc-ph/RSS/jtwc/atcr/1991atcr.pdf.

[8]. United States Agency for International Development. The Bangladesh Cyclone of 1991 (PDF) (Report), United States Agency for International Development, https://pdf.usaid.gov/pdf_docs/Pnadg744.pdf.

[9]. WMO (2020). World's deadliest tropical cyclone was 50 years ago. World Meteorological Organization (WMO), Tags: Tropical cyclones, Disaster risk reduction, published 12 November 2020, member Bangladesh, https://wmo.int/media/news/worlds-deadliest-tropical-cyclone-was-50-years-ago.

[10]. Dunn, G., E. (1962). The tropical cyclone problem in East Pakistan. Mon. Wea. Rev., 91, 83-86.

[11]. Frank, Neil and Husain, S. A. (1971). The deadliest tropical cyclone in history? Bulletin of the American Meteorological Society. American Meteorological Society, volume 52, number 6, page 438-444, June 1971. Bibcode:1971BAMS...52..438F. doi:10.1175/1520-0477(1971)052<0438:TDTCIH>2.0.CO;2.

[12]. Wikipedia (2025a). Template: Deadliest typhoons. https://en.wikipedia.org/wiki/Template:Deadliest_typhoons.

[13]. Courtney, Chris (2018). The Nature of Disaster in China: The 1931 Yangzi River Flood. Cambridge University Press. ISBN 9781108284936, February 15, 2018.

[14]. NOAA (2009). The Worst Natural Disasters by Death Toll (PDF). National Oceanic and Atmospheric Administration, 2009. Retrieved January 2, 2012.

[15]. EM-DAT (2024). The International Disaster Database, https://www.emdat.be.

[16]. Wikipedia (2025b). Typhoon Yagi. https://en.wikipedia.org/wiki/Typhoon_Yagi.

[17]. Wikipedia (2025c). List of the deadliest tropical cyclones. https://en.wikipedia.org/wiki/List_of_the_deadliest_tropical_cyclones.

[18]. Wikipedia (2025d). List of costliest Atlantic hurricanes. https://en.wikipedia.org/wiki/List_of_costliest_Atlantic_hurricanes.

[19]. Seneviratne, S.I., X. Zhang, M. Adnan, W. Badi, C. Dereczynski, A. Di Luca, S. Ghosh, I. Iskandar, J. Kossin, S. Lewis, F. Otto, I. Pinto, M. Satoh, S.M. Vicente-Serrano, M. Wehner, and B. Zhou, 2021: Weather and Climate Extreme Events in a Changing Climate. In Climate Change 2021: The Physical Science Basis. Contribution of Working Group I to the Sixth Assessment Report of the Intergovernmental Panel on Climate Change [Masson-Delmotte, V., P. Zhai, A. Pirani, S.L. Connors, C. Péan, S. Berger, N. Caud, Y. Chen, L. Goldfarb, M.I. Gomis, M. Huang, K. Leitzell, E. Lonnoy, J.B.R. Matthews, T.K. Maycock, T. Waterfield, O. Yelekçi, R. Yu, and B. Zhou (eds.)]. Cambridge University Press, Cambridge, United Kingdom and New York, NY, USA, pp. 1513–1766, doi:10.1017/9781009157896.013.

[20]. Citynoise at English Wikipedia (2008). Tropical Cyclones, 1945–2006. Data from the Joint Typhoon Warning Center and the U.S. National Oceanographic and Atmospheric Administration. Colors based on Template talk: Storm colour. By Citynoise at English Wikipedia, CC BY-SA 3.0, March 2008. https://commons.wikimedia.org/w/index.php?curid=18049077.

[21]. Wikipedia (2025e). Impact of hurricanes on Caribbean history. https://en.wikipedia.org/wiki/Impact_of_hurricanes_on_Caribbean_history.

[22]. Church, Christopher (September 2017). "Hurricane Katrina and its Antecedents" (Document). University of Nevada, Reno.

[23]. Church, Christopher (August 2017). "Environmental History: An Introduction" (Document). University of Nevada, Reno.

[24]. IBTrACS (2025). 1998 Major Hurricane MITCH (1998295N12284). International Best Track Archive for Climate Stewardship (IBTrACS). https://ncics.org/ibtracs/index.php?name=v04r01-1998295N12284.

[25]. Quiring, S., Schumacher, A., Labosier, C., and Zhu, L. (2011): Variations in mean annual tropical cyclone size in the Atlantic. J. Geophys. Res., 116, D09114, doi:10.1029/2010JD015011, 2011.

[26]. DHI (2025). MIKE21 Cyclone Wind Generation Tool, Scientific Documentation, DK-2970, Hørsholm, Denmark, 2024.

[27]. Wikipedia (2025f). Hurricane Mitch. https://en.wikipedia.org/wiki/Hurricane_Mitch.

[28]. Sanoxel (1998). Track map of Hurricane Mitch of the 1998 Atlantic hurricane season. File: Mitch 1998 path.png. Created by Sanoxel using Wikipedia:WikiProject Tropical cyclones/Tracks. The background image is from NASA. Tracking data is from the National Hurricane Center.

[29]. Young, I.R. and Sobey, R.J. (1981). The numerical prediction of tropical cyclone wind-waves. James Cook University of North Queensland, Townville, Dept. of Civil & Systems Eng., Research Bulletin No. CS14.
[30]. Holland, G. (1980). An analytic model of the wind and pressure profiles in hurricanes. Monthly weather review, volume 108, pp. 1212-1218.
[31]. WMO (2008). Guidelines for converting between various wind averaging periods in tropical cyclone conditions, Appendix II, World Meteorological Organisation (WMO), October 2008.
[32]. Shore Protection Manual (1984). Department of the Army, US Army Corps of Engineers, Washington, DC 20314.
[33]. Harper, B.A., Hardy, T.A., Mason, L.B., Bode, L., Young, I.R., Nielsen, P. (2001). Queensland climate change and community vulnerability to tropical cyclones. Ocean Hazards Assessment – Stage 1, Report, Department of Natural Resources and Mines, Queensland, Brisbane, Australia, 368 p.
[34]. Sobey, R.J., Harper, B.A. and Stark, K.P. (1977). Numerical simulation of tropical cyclone storm surge. Research Bulletin CS-14, Dept Civil and Systems Engineering, James Cook University.